Chalmers University of Technology

Direct air capture for flue gas stream with low CO_2 concentration

Feasibility assessment of direct air capture for removing CO_2 from low CO_2 concentration flue gas streams

Master's thesis at Energy Technology department in Sustainable Energy Systems Program

RISHABH VISHWANATHA

DEPARTMENT OF SPACE, EARTH AND ENVIRONMENT
CHALMERS UNIVERSITY OF TECHNOLOGY
Gothenburg, Sweden 2022
www.chalmers.se

Master's thesis 2022

Direct air capture for flue gas stream with low CO_2 concentration

Feasibility assessment of direct air capture for removing CO_2 from low CO_2 concentration flue gas streams

RISHABH VISHWANATHA

CHALMERS
UNIVERSITY OF TECHNOLOGY

Department of Space, Earth and Environment
Division of Energy Technology
Chalmers University of Technology
Gothenburg, Sweden 2022

Direct air capture for flue gas stream with low CO_2 concentration
Rishabh Vishwanatha

Supervisors: Sina Hoseinpoori, Tharun Roshan Kumar, Department of Space, Earth and Environment
Examiner: David Pallarès, Department of Space, Earth and Environment

Master's Thesis 2022
Department of Space, Earth and Environment
Division of Energy Technology
Chalmers University of Technology
SE-412 96 Gothenburg
Telephone +46 31 772 1000

Cover: Solid sorbent adsorption DAC plant (Source: Climeworks)

Typeset in LaTeX
Printed by Chalmers Reproservice
Gothenburg, Sweden 2022

Direct air capture for flue gas stream with low CO_2 content
Process modelling of DAC for flue gas stream from process/manufacturing industry with low CO_2 content
Rishabh Vishwanatha
Chalmers University of Technology

Abstract

Direct air capture (DAC) and storage is a technology that helps yielding negative CO_2 emissions. This technology's main objective is to reach the UN climate goals. The advantage of DAC over other traditional post combustion carbon capture technology is that it can capture CO_2 from a stream where the CO_2 concentration is very low (0.04%, atmospheric concentration).
The aim of this thesis to assess if DAC technology can be used to capture CO_2 from a manufacturing plant with very low(1%) CO_2 concentration. Two promising technologies of DAC are explored in this thesis: High temperature absorption and Low temperature adsorption. First, a process model is developed for both the technologies to evaluate system for the required concentration.
Then a techno-economic comparative analysis is conducted. From the results of this thesis, it is seen that the absorption process consumed more energy when compared to adsorption process. The absorption process also has a higher total levelized cost of CO_2 captured when compared to adsorption process.

Keywords: Adsorption DAC, Absorption DAC.

Acknowledgements

I would firstly like to thank my examiner David Pallarès, for giving me the opportunity to work on an extremely interesting thesis, for assisting me in resolving serious team related issues (which were a lot) and to always be welcoming when I had personal issues as well. I also want to thank him for providing really good ideas and valuable inputs. I would also finally like to thank him for all the opportunities he has given me during the course of my master's program.

I would like to thank both Sina Hoseinpoori and Tharun Roshan Kumar for their extremely valuable inputs for this thesis. For all the discussions and group works. For continuously providing me the motivation required to keep moving forward during this thesis work.

I would like to thank Volvo cars and Charlotte Bergek for always keeping an open conversation and for providing me with the data and financial support to complete this thesis work.

I would like to thank my parents Geeta and Vishwanatha for their continued support and go for it attitude that they have instilled in me in every aspect of my life.

Finally I would like to thank my girlfriend Harsha for continuously supporting me and standing like a rock beside me through all the personal ups and downs during this thesis work.

Rishabh Vishwanatha, Gothenburg, June 2022

List of Acronyms

Below is the list of acronyms that have been used throughout this thesis listed in alphabetical order:

ASU	Air Separation Unit
AUX	Auxiliary Units
BEC	Bear Erected Cost
BET	Brunauer-Emmett-Teller
CAPEX	Capital Expenditure
CCS	Carbon Capture and Sequestration
CFB	Circulating Fluidized Bed
DAC	Direct Air Capture
EPC	Engineering, Procurement and Construction Cost
GAB	Guggenheim-Anderson-de Boer
GHG	Green House Gases
HSRG	Heat Recovery Steam Generator
LC	Labour Cost
MC	Material Cost
NG	Natural Gas
OPEX	Operational Expenditure
TDFC	Total Direct Field Cost
TFC	Total Field Cost
TPC	Total Plant Cost
VTSA	Vacuum Temperature Swing Adsorption

Contents

List of Figures

List of Tables

1

Introduction

1.1 Background

Climate change is a critical global issue that is part of our world, which is caused by increased levels of greenhouse gases (GHG) in the atmosphere. Today, average carbon dioxide (CO_2) concentration in the atmosphere is 421 ppmv[2], i.e., about 0.04 volume percent, equivalent to an atmospheric reservoir of about 3200 $GtCO_2$ [7]. To address the increase in global CO_2 emissions to the atmosphere, GHG emission reduction targets and a wide range of greenhouse gas mitigation technologies are being considered, such as carbon capture from flue gases at power plants and other industrial sites followed by transportation to long-term geological storage [7].

Capturing of CO_2 from air is a very old process. It has been used from a long time only for different purposes at different periods. In 1950s CO_2 capture from ambient air was commercialized as a pre-treatment for cryogenic air separation[12].Then in the 1960s, CO_2 capture from air was considered as a feed stock for production of hydrocarbon fuels using mobile nuclear power plants[12]. In the 1990s, Klaus Lackner for the first time explored DAC as a technology for large scale CO_2 capture to mitigate climate risk[12]. In 2015 carbon engineering set up their first large scale absorption DAC pilot plant in Squamish, Canada. This is a high temperature absorption plant which is one of the processes in the scope of this thesis. In 2017 Climeworks commissions world's first commercial-scale DAC plant in Switzerland. This is a low temperature adsorption process which is the second process that is in the scope of this thesis.

Direct air capture (DAC) is one pathway among the negative emissions technologies to capture CO_2 directly from the air. DAC should be deployed to achieve emission trajectories in line with the net zero CO_2 emission objective and climate change mitigation [23]. Indeed, DAC is expected to play a key role in the transition to a net-zero system, in particular, to offset the emissions of industrial sectors that are difficult to decarbonize [23]. National and international mandates on emission reduction have made carbon capture from industrial emission sources an essential pillar of the technological development of our society.

This thesis is trying to bring into attention that manufacturing plants still emitting CO_2 at «4% concentration. For example, Paint shops of automotive assembly plants[3][19]. They are the largest consumers of energy and emitter of atmospheric emissions. LPG is used for boiling and burning processes and diesel is used as fuel

for forklifts [3][19]. The emissions are present but the concentrations of CO2 is too low for traditional post-combustion CCS technology. Traditional post-combustion CCS technology is commonly applied at point sources of CO_2 which are 4% and above. There there´is DAC technology which removes CO_2 from atmosphere (CO_2 concentration of 0.04%). This thesis asses the feasibility of removing CO_2 from manufacturing plant flue gas lines using DAC technology.

1.2 Aim and scope

This thesis assesses the suitability of two different DAC technologies to remove CO_2 from low concentration («4%) industrial streams: Aqueous sorbent high-temperature process and solid sorbent low-temperature process are checked both technically and economically. More specifically, the thesis will also answer the following questions.

- Do the two processes function at CO_2 concentrations «4% (manufacturing plant conditions)?
- Which of the two processes consumes less specific energy?
- Which of the two technology benefits from economy of scale when capturing CO_2 from manufacturing flue gas streams?

2

Theory

This section describes the two DAC processes considered: the absorption, and the adsorption process.

2.1 Absorption process

The absorption process (see **figure2.1**) starts with absorbing CO_2 in the air contactor[12]. Air contactor is based on commercial cooling tower technology, and the design benefited from close collaboration with SPX cooling technology, a leading vendor[12]. Even though the geometry and the fluid chemistry is different when compared to a conventional tower, it has many of the same components such as fans, structured packings, demisters, fluid distribution systems, and fiber-reinforced plastic structural components[12]. Absorption using air contactor is done by allowing the ambient air to flow over a film of aqueous sorbent KOH solution, which produces K_2CO_3. The K_2CO_3 solution flows into the pellet reactor where it reacts with $Ca(OH)_2$ to form $CaCO_3$ and KOH. $CaCO_3$ is sent to calciner to undergo calcination reaction to get pure CO_2 . CO_2 is then sent to compressor for compresson and CaO is sent to slaker for hydration into $Ca(OH)_2$.

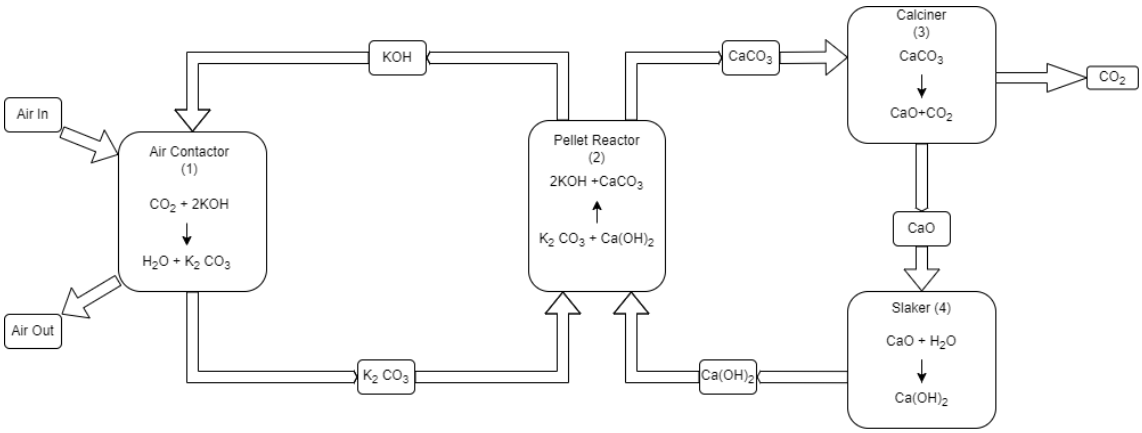

Figure 2.1: Absorption process chemistry

2.1.1 Alkali capture of CO_2

In a preliminary reaction in the air contactor (see **figure2.1**), air with 400 ppm concentration of CO_2 comes in contact with 2.0M KOH solution. Large fans/blowers run to bring in the ambient air into the contactor where there is KOH liquid film with a characteristic e-folding length of 0.3µm [12]. The air comes in contact with

the film which results in OH^- ion transfer with CO_3^{2-} ion resulting in formation of K_2CO_3 and H_2O. K_2CO_3 is sent to Pellet reactor[12]. This is an exothermic reaction hence, it generates 95.8 kJ/mol of heat. The most influencing factors for loading (K_L(mol/mol)) of CO_2 on KOH solution, which is calculated using **equation 5.2**[13] depends on [OH-] concentration and the temperature[12] of the KOH solution. The relationship of solution concentration, temperature and pressure with K_L is show in **Figure 2.2**, **Figure 2.3** and **Figure 2.4** respectively which is got from experimental results of [13]. From **Figure 2.2** we can see that as the concentration of KOH solution increases, CO_2 loading decreases. Hence, it is optimal to keep the concentration of KOH solution as low as possible for high K_L. From **Figure 2.3** we can see that with increase in temperature the CO_2 loading decreases. Hence, it is optimal to maintain the temperature as low as possible to increase the K_L. From **Figure 2.4** we can see that the with increasing partial pressure of CO_2 there is an increase in the K_L. Hence it is preferred to have high partial pressure/ concentration of CO_2 in te flue gas from which Carbon capture is taking place. Typical K_L for CO_2 is 1.3 mm/s at 20°C [12]. The KOH solution composition is 1.0M OH^-, 0.5M CO_3^{2-} and 2.0M K^+[12]. The complete reaction is shown in **Equation 2.1**.

$$CO_{2(g)} + 2KOH_{(aq)} \rightarrow H_2O_{(l)} + K_2CO_{3(aq)} - 95.8kJ/mol \tag{2.1}$$

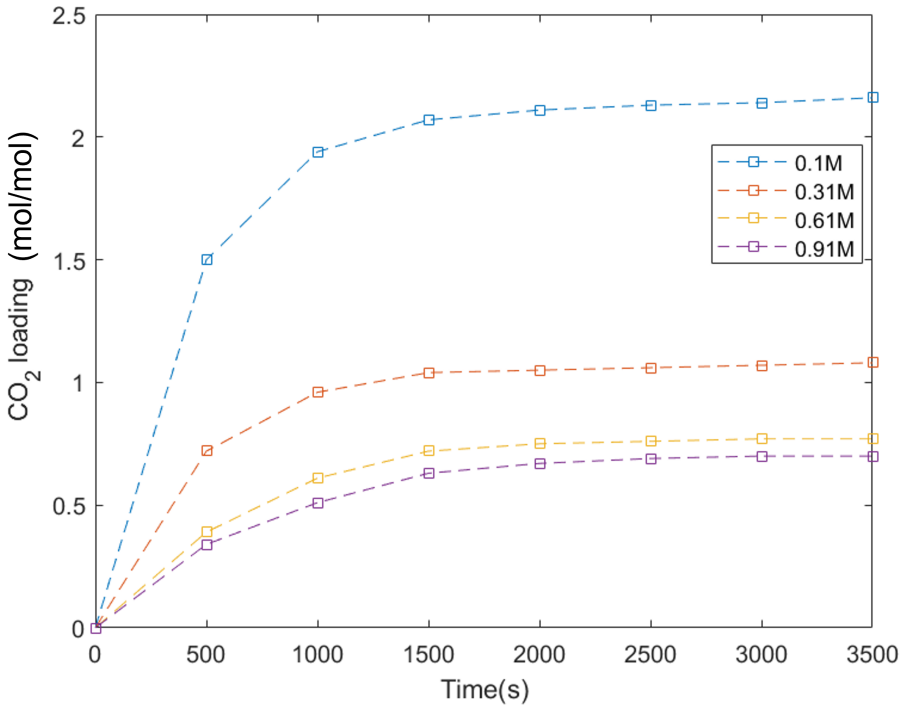

Figure 2.2: Dynamic CO_2 loading on KOH solution for varying KOH concentration [13]

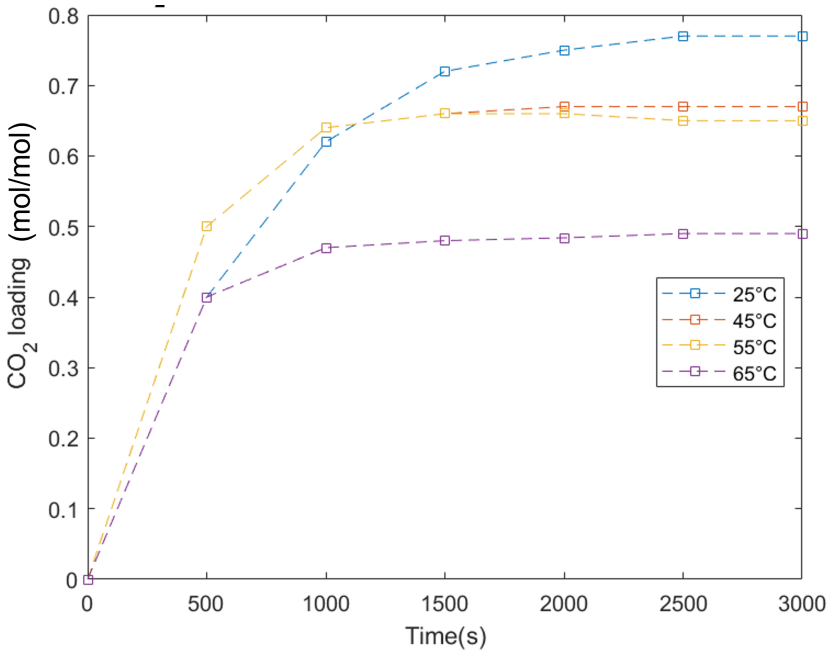

Figure 2.3: Dynamic CO_2 loading on KOH solution for varying temperature of input gas [13]

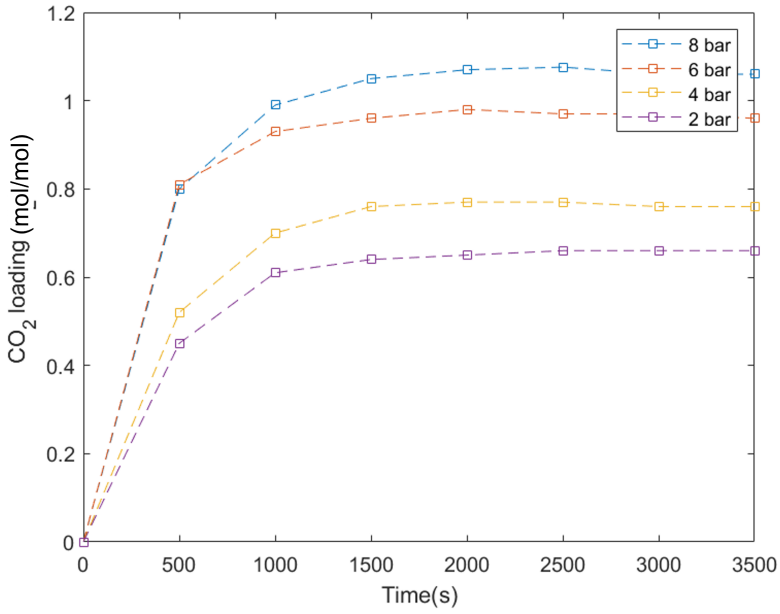

Figure 2.4: Dynamic CO_2 loading on KOH solution for varying partial pressure of CO_2 in input gas[13]

2.1.2 Causticization reaction

Carbonate ion is removed from the K_2CO_3 solution by causticization in pellet reactor as shown in **equation 2.2**. This reaction occurs in a circulating fluidized bed reactor [12]. 0.1-0.9 mm diameter $CaCO_3$ pellets are suspended in K_2CO_3 solution that flows upwards at 1.1-2.5cm/s. A slury of 30% $Ca(OH)_2$ is injected into the bottom

of the reactor vessel[12]. As Ca^{2+} reacts with CO_3^{2-} it drives dissolution of $Ca(OH)_2$ and precipitation of $CaCO_3$, but the fraction of Ca^{2+} that is precipitated onto the pellets depends on maintaining high surface area of the pellets [12]. This results in KOH regeneration and recirculating it back to the air contactor. The $CaCO_3$ is sent further to calciner.

$$K_2CO_{3(aq)} + Ca(OH)_{2(g)} \rightarrow 2KOH_{(aq)} + CaCO_{3(s)} - 5.8kJ/mol \tag{2.2}$$

2.1.3 Calicantion

The $CaCO_3$ is sent to a calciner to undergo calcination reaction for producing CO_2 as shown **equation 2.3**. This is accomplished in an oxygen fired CFB [12]. The $CaCO_3$ pellets undergo dissociation reaction. This is an endothermic reaction (Δh=178.3kJ/mol). Heat is provided by combustion of natural gas/ biogas in the presence of O_2[12]. This heat can also be various other sources as well, as a replacement for natural gas, eg. electrification. The dissociation reaction results in CaO formation which is further sent to Slaker and CO_2 is sent for compression. Once sent to sequestration, CO_2 can be sent to other industries (eg. cement industry, steel industry, etc.) based on their requirement.

$$CaCO_{3(s)} \rightarrow CaO_{(s)} + CO_{2(g)} 178.3kJ/mol \tag{2.3}$$

2.1.4 Slaking

For regeneration of $Ca(OH)_2$, CaO is sent for slaking. Slaking is an exothermic process (Δh=-63.9) kJ/mol. Here, the CaO is coming in to the slaker from calciner for hydration. CaO slaking requires steam for the hydration reaction. The steam required for slaking reaction is produced by preheating the wet $CaCO_3$ pellets coming in from pellet reactor hierarchy's wash tank. The objective of washing the $CaCO_3$ pellets is to have low alkali carryover which allows the use of CFB rather than rotary klin [12]. The steam is used for slaking CaO to finally get $Ca(OH)_2$. The $Ca(OH)_2$ is recirculated back to the pellet reactor. The complete slaking reaction reads:

$$CaO_{(s)} + H_2O_{(l)} \rightarrow Ca(OH)_{2(s)} - 63.9kJ/mol \tag{2.4}$$

2.1.5 Thermodynamic model/package

The property method used in the model is ENRTL-RK which is based on unsymmetric electrolyte NRTL property model. It uses

- The Redlich-Kwong equation of state for vapor phase properties
- The unsymmetric reference state (infinite dilution in aqueous solution) for ionic species.
- Henry's law for solubility of supercritical gases.
- Unsymmetric electrolyte NRTL method of handling zwitterions

The Redlich-Kwong equation of state can calulate vapor phase thermodynamic properties. It is applicable for systems at low to moderate pressures (maximum pressure 10 atm) for which the vapor-phase nonideality is small. The equation reads[14]:

$$p = \frac{RT}{V_m - b} - \frac{a/T^{0.5}}{V_m(V_m + b)} \tag{2.5}$$

The Henry's constant model is used when Henry's law is applied to calculate K-values for dissolved gas components in a mixture. Henry's law is available in all activity coefficient property methods.The model calculates Henry's constant for a dissolved gas component (i) in one or more solvents (A or B). The base equation reads [20]:

$$\ln(H_i/\gamma_i^{\infty}) = \sum_A w_A \ln(H_{iA}/\gamma_{iA}^{\infty}) \tag{2.6}$$

2.2 Adsorption process

The overview of a generic adsorption cycle can be understood by observing **Figure 2.5**.The adsorption phenomena are schematically divided into two large families according to the nature of the bonds between the adsorbate and the solid[21]. These are:
Physisorption (weak interaction), eg. on activated carbons, activated aluminas, silica gels or zeolites, and chemisorption (strong interaction), e.g., on chemical adsorbents based on amines immobilized on a solid support or alkali carbonates.
Chaemisorption: An optimal adsorbent would combine the following qualities: high adsorption capacity, high selectivity, easily regenerable, fast kinetics, high resistance (mechanical, chemical, and thermal) and lifetime, high availability, low pressure drop, low toxicity, and low cost[21]. In practice, a major limitation of physical adsorbents is their low adsorption capacity at low CO_2 partial pressure, which leads to a preferable use of chemical adsorbents for CO_2 capture from air[21]. On the other hand, chemical adsorbents have a higher adsorption capacity compared to physical adsorbents, the energy consumption associated with their regeneration is higher for breaking the chemical bonds between the adsorbate and the adsorbent[21]. The use of an amine bonded to a porous solid support, e.g., such as honeycomb monoliths, pellets, or other granular shapes, is therefore suitable.
Hence, a chemisorption-based adsorbate is used in this thesis with vacuum temperature swing process to adsorb both CO_2 and H_2O from air.

2.2.1 Amine-functionalised adsorbents

In adsorption process, both CO_2 and H_2O are co-adsorbed onto an amine-fictionalised adsorbent Lewatit VP OC 1065. Adsorption equillibrium of species onto a solid surface is typically described by isotherms function which are functions of temperature and partial pressure of the specific species(CO_2, H_2O, etc.).

2.2.1.1 CO_2 isotherm

A standard isotherm used to describe CO_2 adsorption onto a amie-functionalised adsorbents is the temperature-dependent Toth isotherm which has previously been used for amine functionalised silica, cellulose, and Lewatit VP OC 1065 [21]. Toth isotherm is an extension of Langmuir isotherm with improved fit factor at lowest and highest pressure ranges [18], the lowest region being specifically relevant for amine functionalized sorbents due to their high affinity for CO_2 [21]. The equation

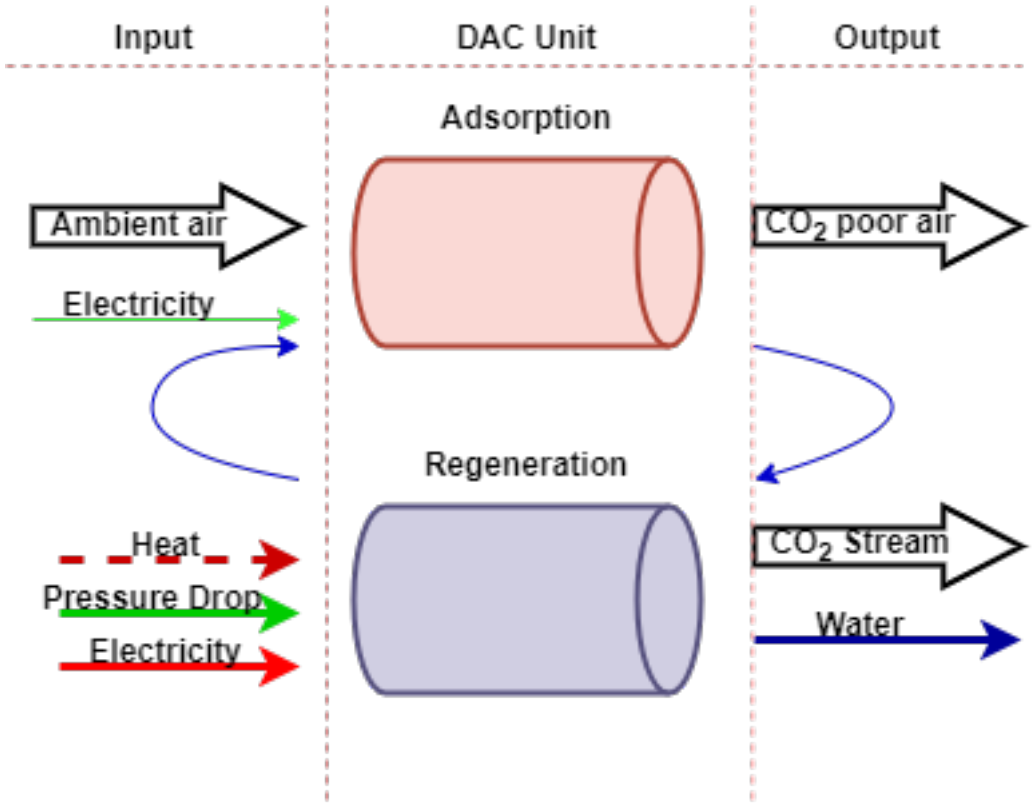

Figure 2.5: Adsorption process[8]

for defining the temperature-dependent form of the Toth isotherm reads:

$$q_{CO_2}(T, p_{CO_2}) = \frac{n_s(T).b(T).p_{CO_2}}{(1 + (b(T).p_{CO_2})^{t(T)})^{1/t(T)}} \tag{2.7}$$

where q_{CO_2} denotes the amount of adsorbed CO_2 in equilibrium at a partial pressure of p_{CO_2}, $n_s(T)$ is the maximum adsorbate loading at saturation,b and t are temperature dependent parameter.[9] b,t and n_s are calculated from **Equation 2.8-2.10** respectively.
The affinity of the sorbent to CO_2 is defined by **Equation 2.8** where b_0 [pa^{-1}] is a pre-exponential affinity parameter, $\Delta h_{ads,CO_2,0}$ [J mol^{-1}] is the isosteric heat of adsorption and R [J $mol^{-1}K^{-1}$] is the universal gas constant.

$$b(T) = b_0.e^{\frac{\Delta h_{ads,CO_2,0}}{R.T_0}.(\frac{T_0}{T}-1)} \tag{2.8}$$

The surface heterogeneity parameter is defined in **Equation 2.10** where t_0 is t at reference temperature, and α is a factor used to describe the temperature dependency.

$$t(T) = t_0 + \alpha.(1 - \frac{T_0}{T}) \tag{2.9}$$

Where $n_{s,0}$ [mol kg^{-1}] is n_s at reference temperature T_0[K],T [K] is the temperature, and χ is a factor used to describe the temperature dependency.

$$n_s(T) = n_{s,0}.e^{\chi.(1-\frac{T_0}{T})} \tag{2.10}$$

Toth isotherm derived for various temperatures and partial pressure of CO_2 and can be seen in **figure 2.6**:

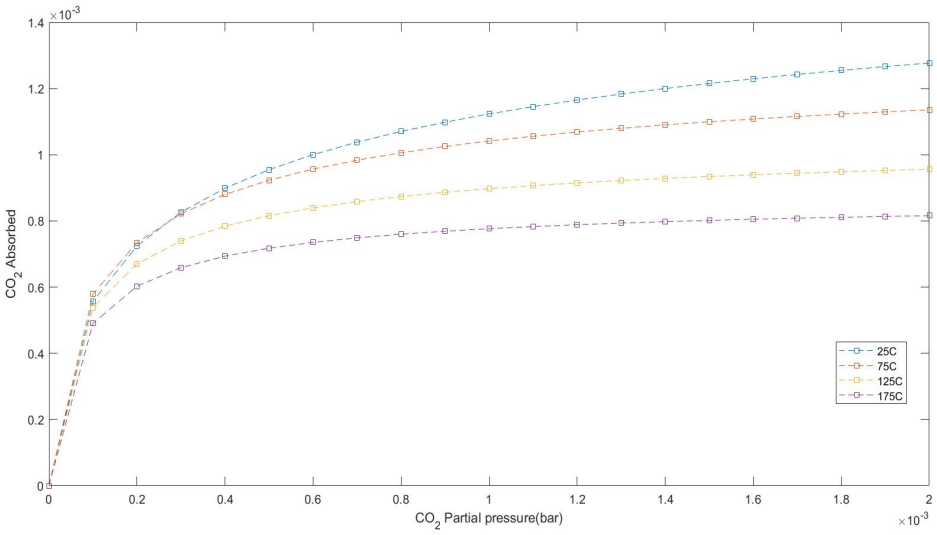

Figure 2.6: Loading curve of CO_2 on Amine cellulose adsorbent[21]

2.2.1.2 H_2O isotherms

Adsorption of water onto Lewatit®VP OC 1065 follows a type III isotherm. Guggenheim-Anderson-de Boer (GAB) model was chosen as the isotherm model for H_2O adsorption. This model is an extension of widely used Brunauer-Emmett-Teller (BET) model [21]. There are a number of assumptions when it comes to the BET equations. The BET assumes that the first layer of adsorption has a heat of adsorption that is different from every subsequent layer, but the subsequent layers have a heat of adsorption equivalent to the latent heat of condensation [21]. On the other hand the GAB model improves this by assuming that only after 10th layer the heat of adsorption is equal to the latent heart of condensation. The 2nd and 9th layers have a heat of adsorption that is different from the first layer [21]. The GAB isotherm reads:

$$q_{H_2O} = \frac{q_m kcx}{(1-kx)(1+(c-1)kx)} \tag{2.11}$$

Where q_{H_2O} [mol kg^{-1}] is the loading of water, q_m [mol kg^{-1}] is the loading that corresponds to the monolayer, k and C are the affinity parameters, and x is the relative humidity. k and c have temperature dependency according to Anderson,s derivation [21]. The relationship can be seen in **Equations 2.12 2.13**

$$c = \exp\left(\frac{E_1 - E_{10+}}{RT}\right) \tag{2.12}$$

where E_1 [J mol^{-1}] is the heat of adsorption of the first layer of adsorption, and E_{10+} [J mol^{-1}] is the heat of adsorption of the 10th layer and higher, which is the equivalent to the latent heat of condensation of water.

$$k = \exp\left(\frac{E_{2-9} - E_{10+}}{RT}\right) \tag{2.13}$$

where E_{2-9} [J mol^{-1}] is the heat of adsorption of the 2nd to 9th layer.

In the thesis it is decided to incorporate the temperature dependency as the reference case results of the model is validated with experimental results of [21]. which shows temperature dependency, it also takes into consideration the relative humidity dependency. The heat of adsorption of 10th and above layers reads:

$$E_{10+} = -44.38T + 57220 \tag{2.14}$$

The temperature dependency of heat of adsorption for 1st layer and 2nd to 9th layer reads:

$$E_1 = G - \exp(DT) \tag{2.15}$$

$$E_{2-9} = F + GT \tag{2.16}$$

Where C, D, F, and G are constants. Further values of these constants are explored in the modelling section. Finally, relative humidity is defined by Arden Buck equation [21] shown below in **Equation 2.17**

$$P_{sat} = 611.21\exp\left(\left(18.678 - \frac{T - 273.15}{234.5}\right)\frac{T - 273.15}{T - 16.01}\right) \tag{2.17}$$

Where P_{sat} [Pa] is the saturation pressure at T[K] temperature.
The loading curve of H_2O at varying RH can be seen in **figure 2.7**.

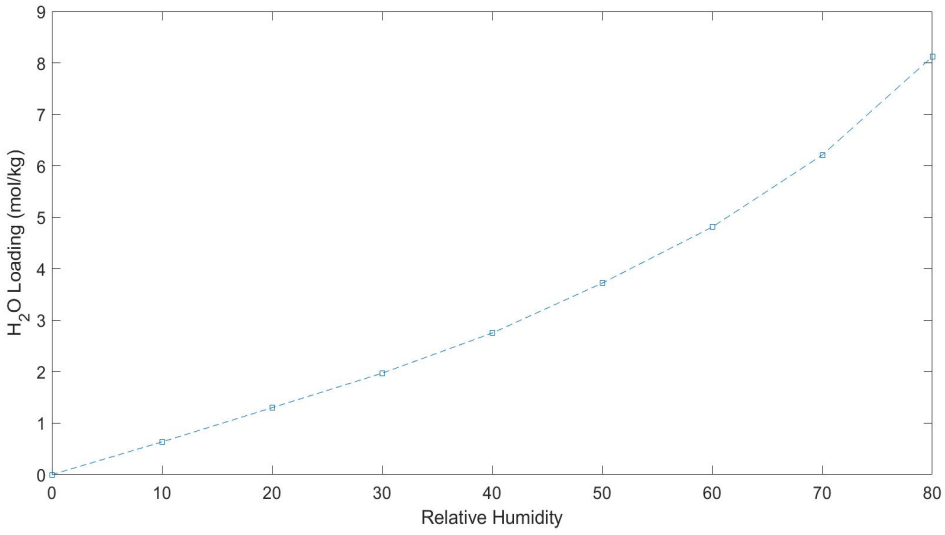

Figure 2.7: Loading curve of H_2O on Lewatit®VP OC 1065 [21]

2.2.1.3 Water-CO_2 co-adsorption isotherm model

Adsorption of CO_2 is affected by adsorption of H_2O but not work [17, 10]. The work in [10] described co-adsorption on an amine-functionalised cellulose material by making adjustments to pure Toth model. The adjustment made are:

$$q_\infty\left(T, q_{H_2O}\right) = q_\infty(T)\left(\frac{1}{1 - \gamma q_{H_2O}}\right) \tag{2.18}$$

$$b\left(T, q_{H_2O}\right) = b(T)\left(1 + \beta q_{H_2O}\right) \tag{2.19}$$

Here γ and β are parameters that describe co-adsorption which is fit to wet experiments conducted in [10].

2.2.1.4 Discretization method

The descritization method used is first order upwind differencing scheme. The first-order (convection) term used is[1]:

$$\frac{\partial \Gamma_i}{\partial z} = \frac{\Gamma_i - \Gamma_{i-1}}{\Delta z}) \tag{2.20}$$

UDS1 has the following advantages(+) and disadvantages (-):

- + Unconditionally stable (does not produce oscillations in the solution)[1]
- + Least simulation time.[1]
- - Only first-order accurate[1]
- - Gives large amount of "false" or numerical diffusion (this problem can be overcome by increasing number of nodes)[1]

2.2.1.5 Momentum balance

Ergun equation is used for momentum balance in the adsorption bed which will be **section 4.2.1.1**. It combines the description of pressure drops by Karman-Kozeny equation for viscous flow and the Burke-Plummer equation for inertial flow. It can be seen in **Equation 2.21** [6]. It is most commonly used in modelling as it has flexibility to be used in both laminar and turbulent gas flow.

$$\frac{\partial P}{\partial z} = \left(\frac{1.5 \times 10^{-3}(1-\varepsilon_i)^2}{(2r_p\psi)^2\varepsilon_i^3}\mu v_g + 1.75 \times 10^{-5} M\rho_g \frac{(1-\varepsilon_i)}{2r_p\psi\varepsilon_i^3} v_g^2 \right) \tag{2.21}$$

Where ψ is sphericity, r_p is particle radius, ε_i is interparticle voidage, μ is dynamic gas viscosity, ρ_g is the gas density, v_g is the superficial velocity and finally M is the molecular weight.

2.2.1.6 Kinetic model

The kinetic model assumed to be used in the adsorption model is the lumped resistance model with a linear driving force it can be seen in **Equation 2.22** [6].

$$\rho_s \frac{\partial w_i}{\partial t} = MTC_{gi}\,(c_i - c_i^*) \tag{2.22}$$

Where MTC_{gi} is the mass transfer coefficient of component í and c_i is the concentration of component i. more detailed explanation about the parameters can be seen in modelling section.

2.2.2 Auxiliary units

The auxiliary units used in the model of adsorption process are blower (to get the flue gas into the adsoprtion bed), vacuum pumps (for creating vacuum within the adsorption bed with a pressure of 0.2 bar), and heater water pump (which is used for circulating water in heater jacket of the adsorption column). The specific work consumption W [$Jmol^{-1}$] calculation for all the three components are given by [21].

$$W_{vac} = \frac{\int_{t_{vac,start}}^{t_{vac,end}} \sum_{i=1}^{N_c} n_i(z=L)\frac{1}{\eta_{vac}}\frac{\gamma_{gas}}{1-\gamma_{gas}} RT(z=L)\left(\frac{P_{ambient}^{\frac{\gamma_{gas}-1}{\gamma_{gas}}}}{P(z=L)} - 1 \right) dt}{N_{CO_2}} \tag{2.23}$$

$$W_{blower} = \frac{\int_{t_{ads,start}}^{t_{ads,end}} \sum_{i=1}^{N_c} n_i(z=0) \frac{1}{\eta_{blower}} \frac{\gamma_{gas}}{1-\gamma_{gas}} RT(z=0) \left(\frac{P(Z=0)^{\frac{\gamma_{gas}-1}{\gamma_{gas}}}}{P_{ambient}} - 1 \right) dt}{N_{CO_2}} \tag{2.24}$$

$$W_{waterpump} = \frac{Q \rho_w g n_w}{100 \eta_{pump}} \tag{2.25}$$

$$W = W_{vac} + W_{blower} + W_{waterpump} \tag{2.26}$$

Where N_c is the number of components $t_{vac,end}$[s] is the time at the end of vacuum step,$t_{ads,end}$[s] is the time at the end of adsorption step, N_{CO_2} is the number of moles of CO_2 captured, γ_{gas} is the heat capacity ratio of the gas,η_{blower} is the blower efficiency, η_{vac} is the vacuum pump efficiency, Q [m] is the head of water in the pump, ρ_w [kgm^{-3}] is the density of water,g [ms^{-2}] is the acceleration due to gravity ,and n_i [$mols^{-1}$] is the mole flow of flue gas.

2.2.3 Sensitivity analysis metric

For comparing the different cases of sensitivity analysis two metrics are used: Capture rate and productivity [$kgm^{-3}h^{-1}$]. Where, capture rate is the ratio of amount CO_2 that is put into the model to the amount of CO_2 captured by the model. Productivity is the ratio of the mass [kg] of CO_2 captured to the volume of the adsorption bed [m^{-3}] and time taken to complete one cycle [h]. Both the metric calculation can be seen in **Equation 2.27** and **Equation 2.28** [21].

$$\text{Productivity} = \frac{m_{CO_2}}{V \times t} \left(kgm^{-3}h^{-1} \right) \tag{2.27}$$

$$\text{Capturerate} = 1 - \frac{m_{outputCO_2}}{m_{inputCO_2}} \tag{2.28}$$

2.3 Techno-economic analysis

To calculate the scaled BEC using reference value, cost curve method is used. The cost curve equation is shown in **equation 2.29**.

$$C_2 = C_1 \left(\frac{S_2}{S_1} \right)^n \tag{2.29}$$

In the above equation
C_2 = Capital cost of the plant with capacity S_2
C_1 = Capital cost of the plant with capacity S_1
Also n = 0.6 according to the "Six-tenths rule"[16] to get a rough estimate of the capital cost if there is not sufficient data available to calculate the index of a particular process.

The direct cost of columns (absorber/desorber/direct contact cooler) with internals (structured packing) are estimated according to:

$$\text{Directcost} = ax^b \tag{2.30}$$

where x is the total volume [m^3] of the column (assuming cylindrical geometry). a and b are constant coefficients. a=91.764 and b=0.6154. The levelized capital cost calculation is obtained by **Equation 2.31**.

$$\text{Levelized} = \text{CI}\left(\frac{\text{CRF}}{\text{U}}\right) \tag{2.31}$$

Where CI [$\$/tCO_2$] is the capital intensity which is the capital cost per unit intensity. CRF is the capital recovery factor is a levelized annual charge on capital divided by the overnight capital cost. and U is the utilisation factor.

3

Methodology

The methodology (see **figure 3.1**) of this works starts with literature survey to understand and get reference cases for each of the two processes. Process modelling is commenced using the reference cases. Once the model is generated, they are validated against reference cases. In case of the abosrption process the reference is Carbon engineering CO_2 capture plant [12] and for the adsorption process, Climeworks is taken as the reference case [21]. Once the validation is completed sensitivity analysis is done to see the effect it has on parameters such as solvent mass flow, Column dimensions, energy usage, heat requirement etc. for both processes. Then a techno-economic analysis is done for each process. Both CAPEX and OPEX cost are calculated giving us the TPC and the levelized cost of capture. The reults of both sensitivity analysis and techno-economc analysis are generated and a conclusion is derived.
Process is modelled using ASPEN plus and ASPEN adsorption. The sensitivity analysis is conducted in ASPEN plus. The economic calculation and some data analysis are performed using MS Excel and Matlab.

3.1 Sensitivity analysis

Once the model is validated against the reference case, sensitivity analysis is performed. Sensitivity analysis was conducted on the model to see the impact it has on the specific energy consumed. The parameters that were varied in the sensitivity analysis were CO_2 capture rate, CO_2 concentration and the mass flow rate of the flue gas. When varying one parameter, other parameters are kept constant at base case values which are: CO_2 concentration - 0.06% [12], CO_2 capture rate - 74.5% [12] and flue gas mass flow rate - 87 t/h (based on the flow rate of flue gas in manufacturing plant). The assumptions made in sensitivity analysis when varying the CO_2 concentration is that with increasing concentration of CO_2 it replaces N_2 in the flue gas.The summary of the sensitivity analysis can be seen in **Figure 3.2**. The reason for choosing these three parameters to be varied for sensitivity analysis is because these govern the electricity consumption and the component sizing for economic analysis. In case 1, CO_2 capture rate is varied in the base case model to see the variation of total energy consumption (GJ/tCO_2). In case 2, CO_2 concentration in the flue gas is varied to check the variation in total energy consumed (GJ/tCO_2).Fianlly, in Case 3, the flue gas total mass flow rate is varied in the base case model to check the variation in total energy consumed (GJ/tCO_2).

Once the adsorption model was validated (see **figure 3.3**, sensitivity analysis was conducted on the model to see what impact it has on the specific energy consumed,

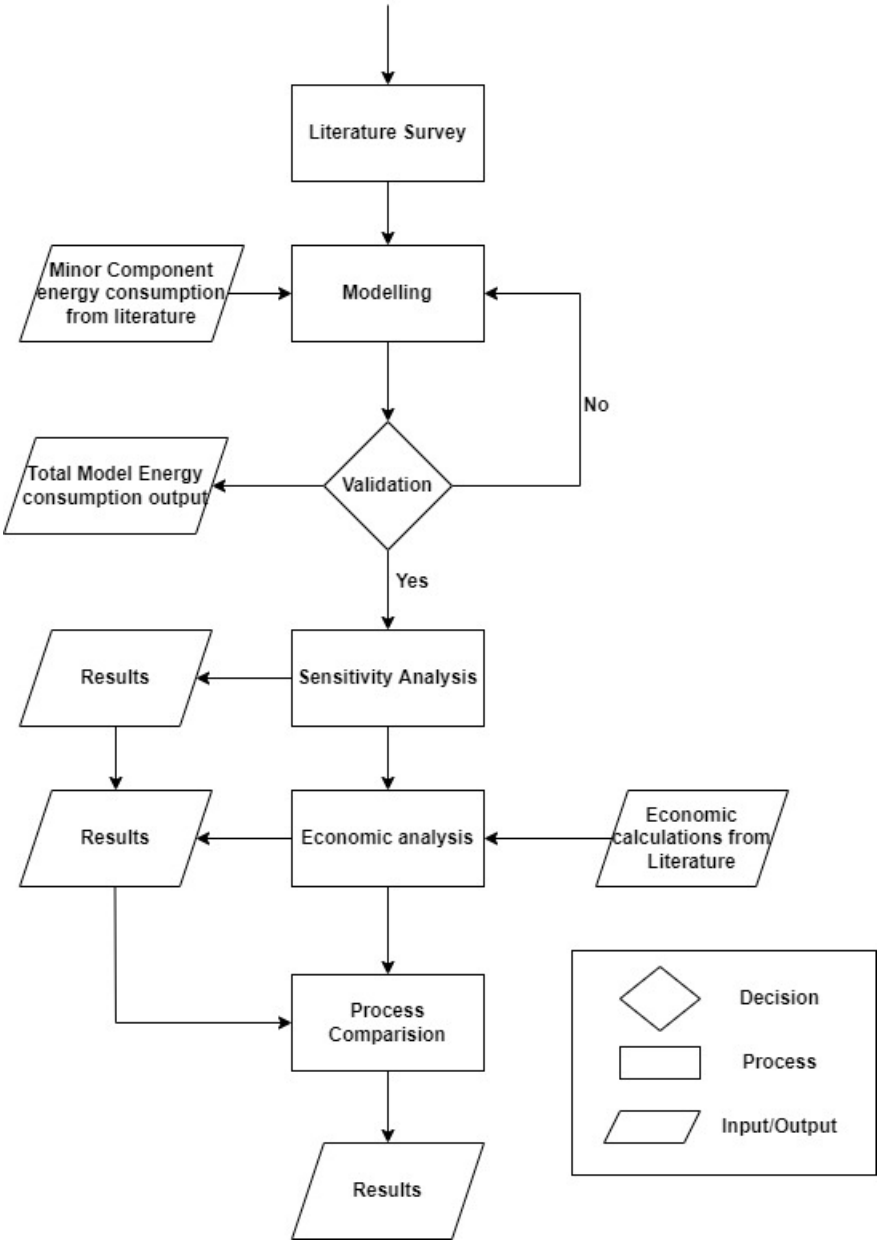

Figure 3.1: Methodology

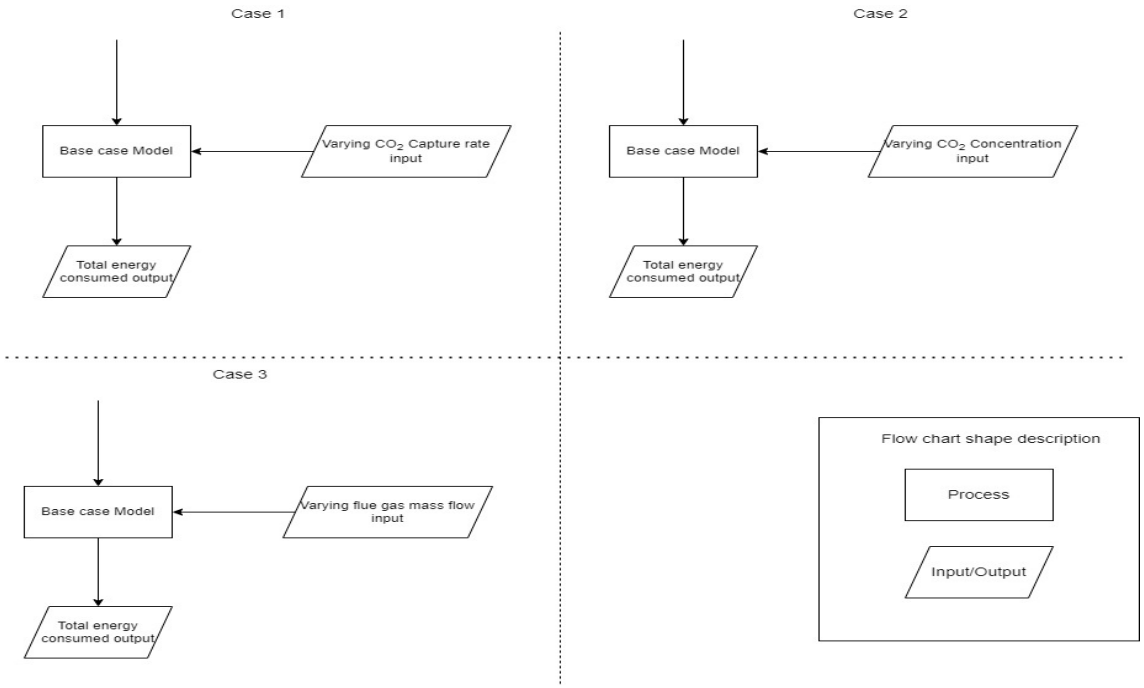

Figure 3.2: Absorption sensitivity analysis

capture rate and productivity of the model. During sensitivity analysis when one parameter is varied the others are kept constant (base case value) as shown in **table 3.1** . The sensitivity analysis was conducted for 3 different values for each parameter and for each concentration of CO_2 in flue gas. The parameters that were varied are Column thickness[m] 0.01m, 0.05m and 0.1m (case 1). Next parameter that was varied was desorption temperature [K] 353.15K, 373.15K and 393.15K (case 2). The maximum desorption temperature that can be used is 393.15K as higher temperatures will destroy the amine based adsorbent used in this model. Next parameter that was varied was CO_2 concentration in the exhaust 20%, 50% and 70% (case 3). The sensitivity was done for 20% as the minimum condition as the adsorption time for 10% concentration at high CO_2 concentration was very small. Finally superficial velocity [m/s] is varied 0.0506 m/s, 0.0606 m/s, 0.0706 m/s (case 4). The maximum superficial velocity was limited to 0.0706 m/s as that is 90% of the minimum fluidization velocity of Lewatit®VP OC 1065 and higher velocities will lead to fluidization of the bed material.

Parameter	**Value**	**Unit**
Column Thickness	0.05	m
Desorption Temperature	373.15	K
CO_2 Concentration in exhaust	10	%
Superficial velocity	0.0706	m/s
CO_2 concentration in flue gas	0.04	%

Table 3.1: Adsorption model base case parameters

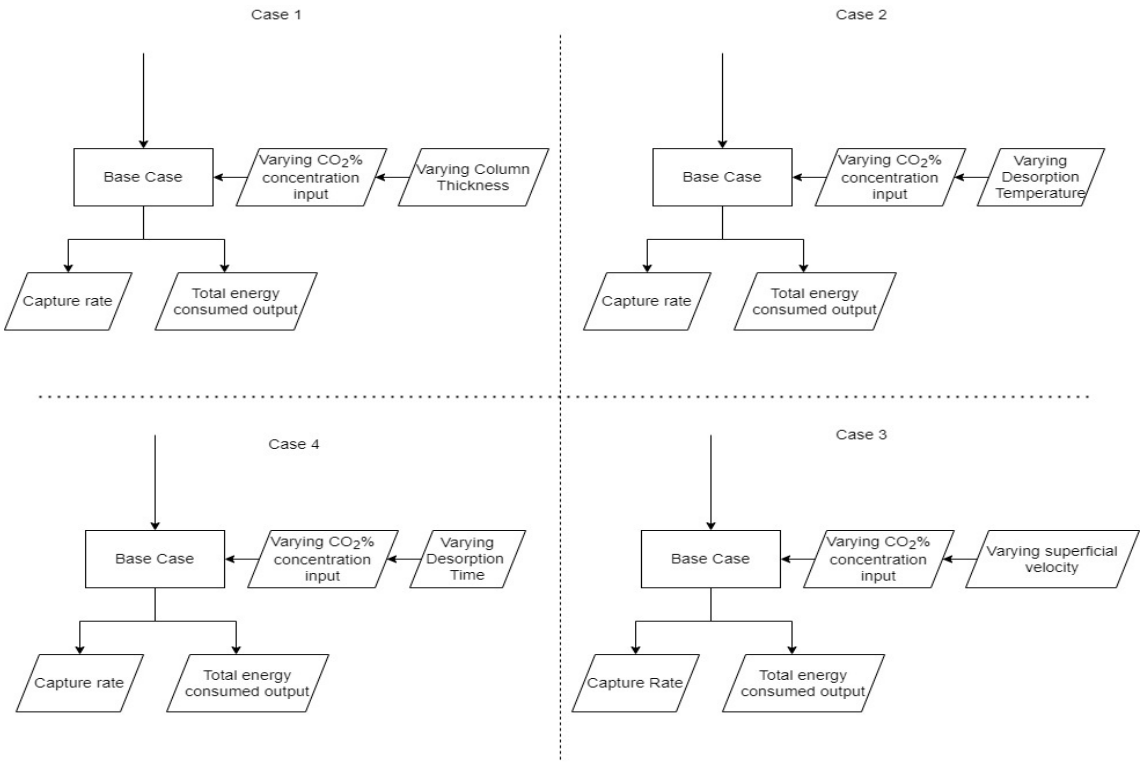

Figure 3.3: Adsorption sensitivity analysis

3.2 Techno-economic analysis

The techno-economic analysis starts with calculation of CAPEX cost which is a bottom-up approach. Generating the CAPEX starts off with getting the bare erected cost(BEC). BEC are either got from literature or using cost functions. Material cost and Labour cost are added to the BEC which gives the total direct field cost (TDFC). The field construction supervision, start-up and commissioning cost which makes up the indirect field cost is added to the TDFC to get total field cost (TFC). Once the TFC is generated, the engineering, procurement and construction cost (EPC) and the contingency cost are added to it. Contingency cost on this project is assumed to have three risk categories which are, project, strategic, and contextual[12]. Strategic risk account for business related issues such as joint venture negotiations, changes in objectives of the project, or changes in resource management, etc[12]. Project risk comprises equipment and supply chain risks along with all site-related risks[12]. Finally the contextual risks are those which are dependent on current laws, geopolitics and economic conditions[12]. This gives the total project/plant cost(TPC). The TPC is utilized in **Equation 2.31** to generate the levelized CAPEX of CO_2 capture. The summary of generating the levelized CAPEX is shown in **Figure 3.4**[12].

Two OPEX cost are taken into consideration. Fixed and variable OPEX cost. Fixed OPEX comprises of make-up stream cost for the lean KOH solution input into the pellet reactor. Variable OPEX cost or energy cost comprises of electricity cost[12]. These two OPEX cost are added to levelized CAPEX cost to generate the total levelized cost.

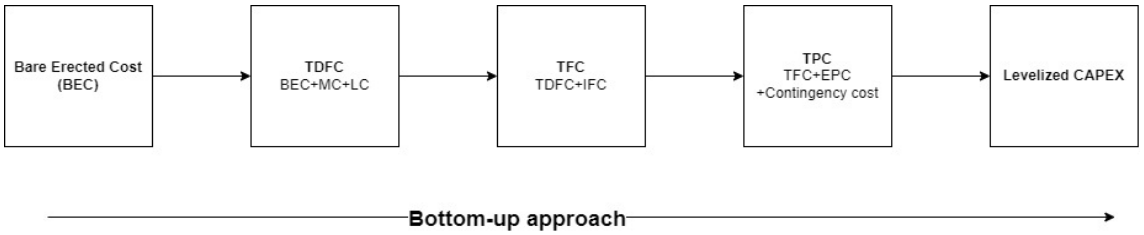

Figure 3.4: Annual CAPEX calculation[12]

The cost curve method is used for all the components of the model except the absorber column as all the other components have the same key parameter for scaling expect absorber column. This is so because air contactor component is used in Keith et.al.[15] for CO_2 capture. Thesis model uses an absorber column for the same purpose. This is because, the flow rate of flue gas in the model is from manufacturing plant (87tph) which is very low when compared to the plant referred to in the reference[15] (251000 tph air in flow). For absorption column, BEC is calculated using power law regression which is shown in **equation 2.30** used in Biermann et.al.[5].

The cost curve method is a type of order of magnitudes estimate, which is a class 5 (concept screening) capital cost estimate without completing a plant design. This method is employed as the thesis works with a first of a kind plant. Therefore it has an accuracy of +100/-20% [16].

4

Modelling

4.1 Absorption Process

4.1.1 Modelling

For absorption process, a pre-existing pilot plant in Canada by Carbon Engineering [12] is used as a reference for validation. while the plant is used to capture CO_2 from the ambient air[12]. model is used to capture low concentration CO_2(1%) from the manufacturing plant's flue gas line. The model is here thus scaled to the flows of a flue gas line from a manufacturing plant. An overview of the absorption process can be seen in **Figure 4.1** where, hierarchy is a terminology used in Aspen plus to represent main sections of the model.

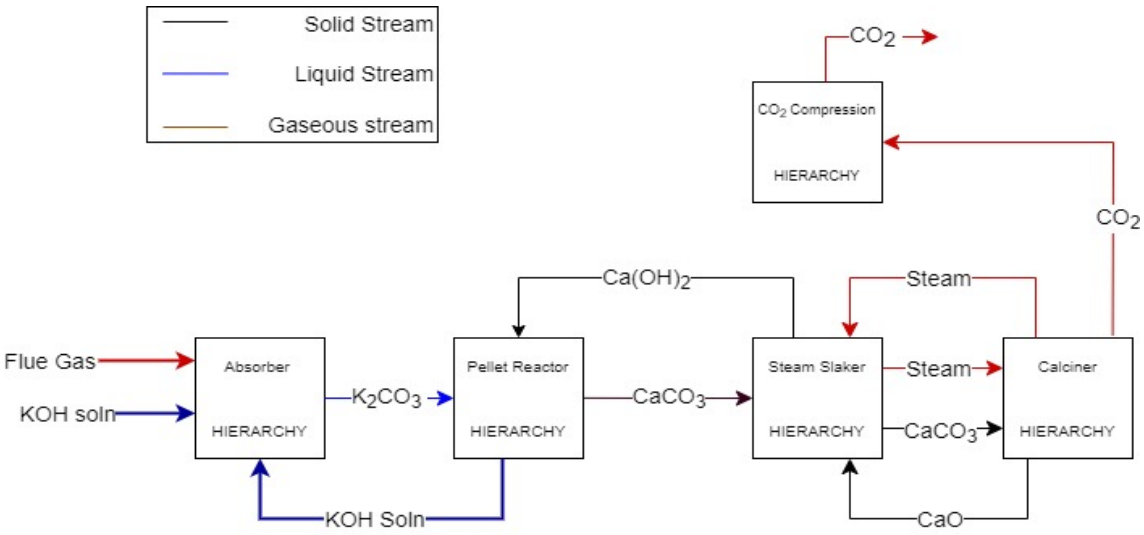

Figure 4.1: Absorption process hierarchy[4]

4.1.1.1 Absorber

Next step is modelling the different hierarchies, which are shown in **Figure 4.1**.The flow rates in the manufacturing plant is very low when compared to the reference case[12] which is designed to capture 1MT CO_2/year, making the air contactor not suitable for our model because of high air inflow requirement. Hence, absorber column is used in the model replacing the air contactor. CO_2 in the incoming flue gas is captured using the aqueous sorbent (1.1M aqKOH). The composition of the flue gas fed to the absorber column can be seen in **Table 4.1**.

Flue gas components	Concentration (%)
N_2	75.96
O_2	23
H_2O	0.98
CO_2	0.06

Table 4.1: Feed flue gas composition[12]

The capture rate of the absorber column has been set to 74.5% [12]. Design spec calculates the required flow rate of KOH using a target CO_2 capture rate (74.5%).

The absorber column has 6 stages, with air entering in stage 1 (bottom of the absorber column) and KOH solution entering in stage 6 (top of the absorber column). Dimension of the absorption column is calculated using Rate based calculation, which is a calculation method which is applied in the ratefrac column, with its defined reaction set in ASPEN plus. It determines the optimum diameter of the absorber column based on the flooding percentage of the limiting stage (stage with maximum flooding). The maximum flooding is set to 80% in this model [12]. Based on the maximum flooding of the limiting stage, the optimized diameter of 4.808m and the length is 12m[12] is derived. The mass flow rate of input air in the model is set according to flows of flue gas in the manufacturing plant (87 t/h).

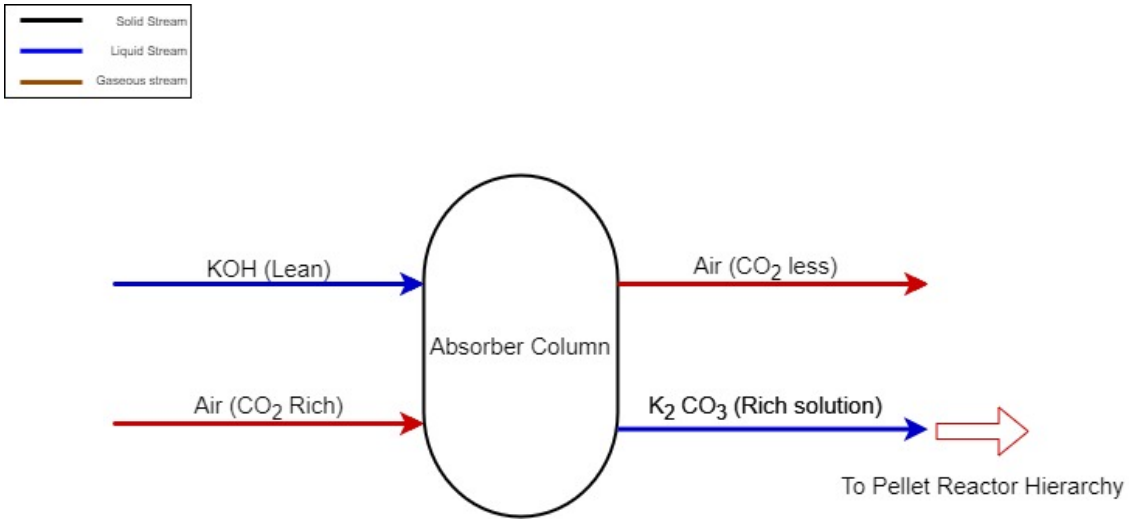

Figure 4.2: Absorber hierarchy

In the reference case an abosrber column is used for CO_2 capture from flue gas of HSRG natural gas turbine. This column has 12 X 7.5 (height X diameter)[12]. The column is filled with 95 m^2/m^3 BERL ceramic packing, with a pressure drop of 1.08 kPa at an average operating gas velocity of 0.75 m/s [12]. The same packing parameters has been used in our model.

4.1.1.2 Pellet reactor

A circulating fluidized bed reactor is used in the pellet reactor hierarchy which results in formation of in$CaCO_3$ pellets [12]. The CFB block in ASPEN plus is not used as there were many unknown parameters hence, a crystaliser block is used. Crystalizer block requires specification of temperature and pressure (25C, 1.01325 bar)[4] and also the saturation calculation method must be provided to perform the crystallization reaction of the compound. However, the chemical reaction has been inserted previously in the property sets section of the software. It is possible to directly refer to the chemistry previously implemented. If it is not done, solubility data or solubility function should be inserted manually in the dedicated section. This block functions in a similar way as a CFB with the same reaction and kinetics.

As shown in **Figure 4.3** the block pellet reactor is fed by four streams. The first stream is the K_2CO_3 solvent that is coming in from the absorber hierarchy. The second stream is the $Ca(OH)_2$ solution which is coming in from the slaker hierarchy. The amount of $Ca(OH)_2$ can be either calculated using a design spec or manually such that all of the 74.5% of CO_2 that is captured in the absorber column is converted into solid $CaCO_3$ pellets, for our case, the amount of CO_2 that is absorbed is 0.0259 t/h and to absorb that, the amount $Ca(OH)_2$ required is 0.114t/h. The third stream being added is a small amount of seed $CaCO_3$ pellets which is used to start the crystallization reaction between K_2CO_3 and $Ca(OH)_2$ to replicate the actual process that occurs in the carbon engineering process [12]. An important factor that needs to be considered in the pellet reactor is calcium retention which is the amount of Ca+ ion that remains in the model throughout the absorption process. It has to be 90%[12]. This is managed by the separator block SEP 2 in **Figure 4.3**). The separator makes sure that 90% of the $CaCO_3$ generated goes into the calciner and the rest 10% is removed from the filter as fines. Now the fines that come out of the filter are split again, where 73.13% $CaCO_3$ is sent to the calciner. 11.5% is disposed, and 15.3% is sent back as seed $CaCO_3$ into the pellet reactor. This ratio of splitting is managed in the model using the splitter block (SPLIT-2). The amount of KOH used in the absorber column to capture 74.5% of CO_2 is sent back to the absorber hierarchy using filter-2 and filter-3. A ratio of solvent in loop to solvent being fed is maintained at 11.114 [12] using a make-up stream. A selector block is used to first run the model using the make-up stream and then switch the input to the pellet reactor from the make-up stream to the loop stream to ensure a smooth running of loop occurs.

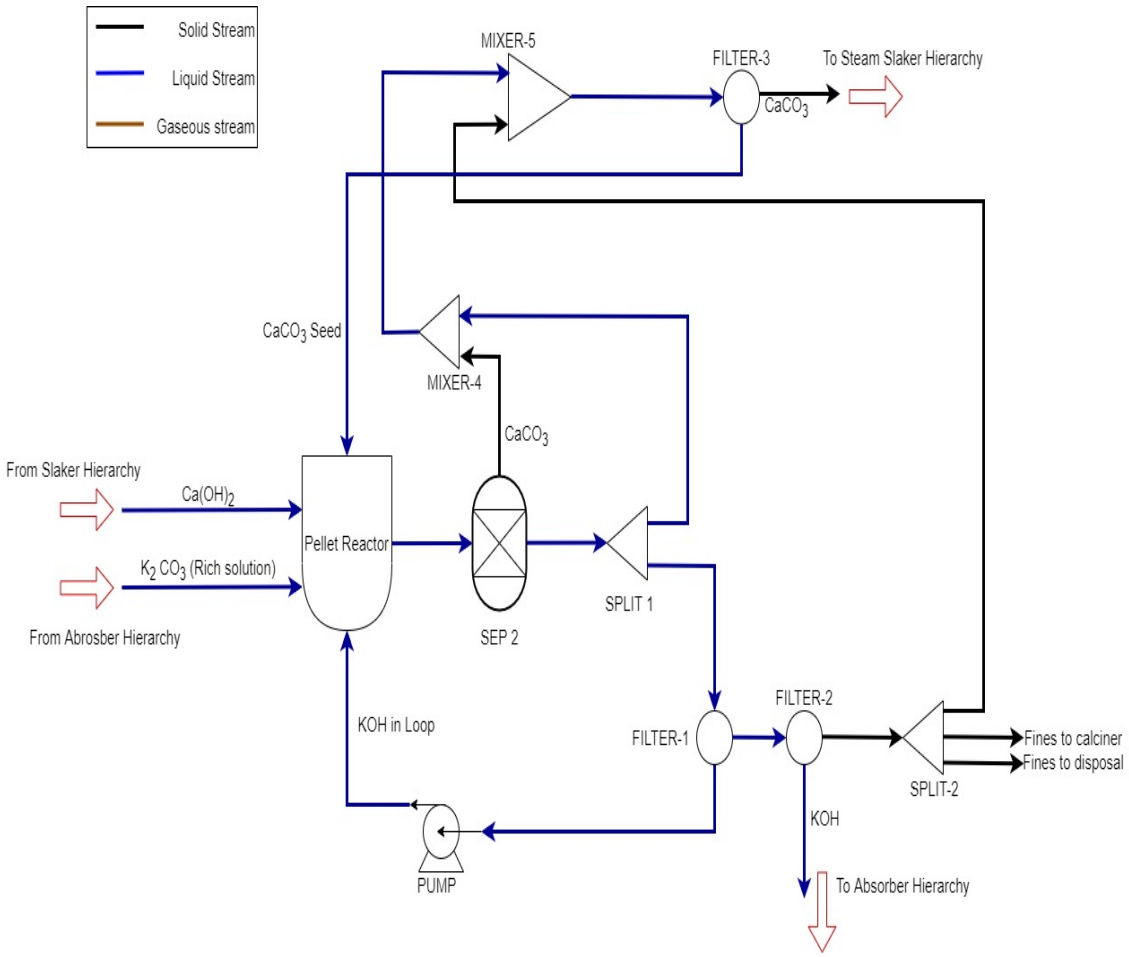

Figure 4.3: Pellet reactor hierarchy [15]

4.1.1.3 Slaker

In the reference case, the slaker is a refractory lined bubbling/turbulent fluid bed that is fluidized by recirculating steam flow[12]. It receives $CaCO_3$ pellets from the washer at ambient temperature and hot CaO at 674°C from the calciner's oxygen preheat cyclone. The fluidized bed has a fluidization velocity of 1 m/s, which transports and slakes quicklime (CaO) particles to form $Ca(OH)_2$. The same process is mimicked in the model using an R-Stoic reactor. For the R-stoic reactor to perform the slaking reaction, the block has to be specified with reaction specification of the slaking reaction as shown in **Equation 2.4**. Hence temperature of 300C and 1 bar pressure is specified in the R-stoic block[12]. The slaking reaction is also specified in the block and a fractional conversion of 0.85 to CaO is used[12].

In the model's slaker hierarchy, there are multiple operations going on. The first one being, washing and drying of $CaCO_3$ pellets that is got from pellet reactor hierarchy, before being sent to the calciner. These pellets are washed in the wash tank with water. The water is supplied from the compressor hierarchy. Once the pellets are washed, the wet pellets are preheated from the heat that is generated from the slaking reaction. This helps evaporating all the water content in the pellets to steam. The primary function of the slaker is to hydrate the CaO got from the calciner. This is an endothermic reaction which converts CaO to $Ca(OH)_2$ in presence of the steam. The steam is generated from heating the $CaCO_3$ pellets. The $Ca(OH)_2$ got from the slaking reaction is sent into the pellet reactor again to keep the double cycle reaction running. Two separators are used in the model to depict the functioning of a fluidized bed's cyclone. There is some amount of un-reacted CaO is sent back to the reactor using the cyclone, and some of the CaO that remains un-reacted are collected in the dust collector and finally disposed off[12]. The secondary use of the steam that is got for heating the $CaCO_3$ pellets is to run a small steam turbine. The electricity generated from this turbine is used to fill some of the energy demand needed for the whole process. The amount of electricity generated from the turbine can be seen in the validation section.

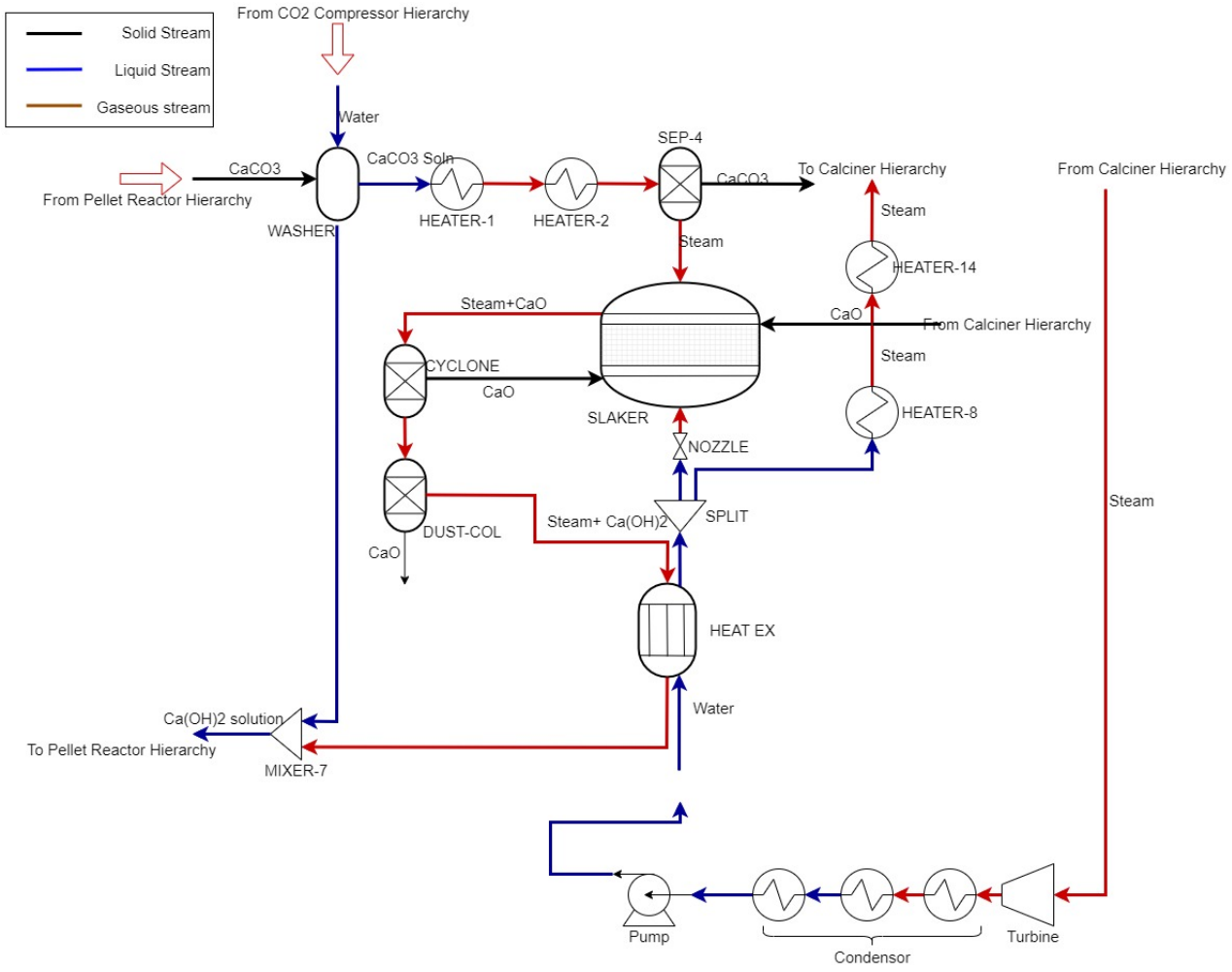

Figure 4.4: Slaker hierarchy [15]

4.1.1.4 Calciner

In the reference case, calcination of $CaCO_3$ to produce CO_2 is accomplished in an oxygen-fired CFB [12]. Carbon Engineering with the help of Technip have deployed high temperature fluidized beds for the same purpose. For example, two 6.7m diameter oxygen clown CFBs used as gold ore roasters in goldstrike mine in Nevada [12].

The calciner, along with the pre-heater cyclones, are large steel vessels lined internally with refractory brick. Fluidized gas is supplied into the bottom of the calciner through a distribution plate made from an arch of refractory, and natural gas is injected directly into the fluidized bed just above the distribution plate using a series of lances[12].

In the model, again an R-Stoic reactor block is used(to replicate this working principle of a calciner). Pre-Heated dry $CaCO_3$ pellets are transferred from the Slaker to the calciner. Within the calciner (circulating fluidized bed reactor) the $CaCO_3$ is broken into CaO and CO_2 through an endothermic calcination reaction. The specifications for the R-stoic reactor block are temperature and the pressure at 900°C and 1 bar respectively[12]. The reactor section of the R-stoic block has two reactions that is specified , reaction 1 being the calcination reaction which is **equation 2.3** and as the calination reaction is an endothermic reaction which requires energy it is got by combusting natural gas (pure CH_4) or biogas with pure oxygen which is specified as reaction 2. The calcination reaction needs 178.3 kJ/mol [12] of heat for the reaction to occur. There are many other alternatives to provide the heat required like electricity, biomethane, etc. Finally, the CaO is sent into the slaker to get slaked lime. The CO_2 that is formed in the calciner comes out at a very high temperature of 900°C which is used to preheat the $CaCO_3$ pellets that are coming into the calciner from the slaker hierarchy using multiple heat exchangers HE-3 and HE-2 in **Figure 4.5**.

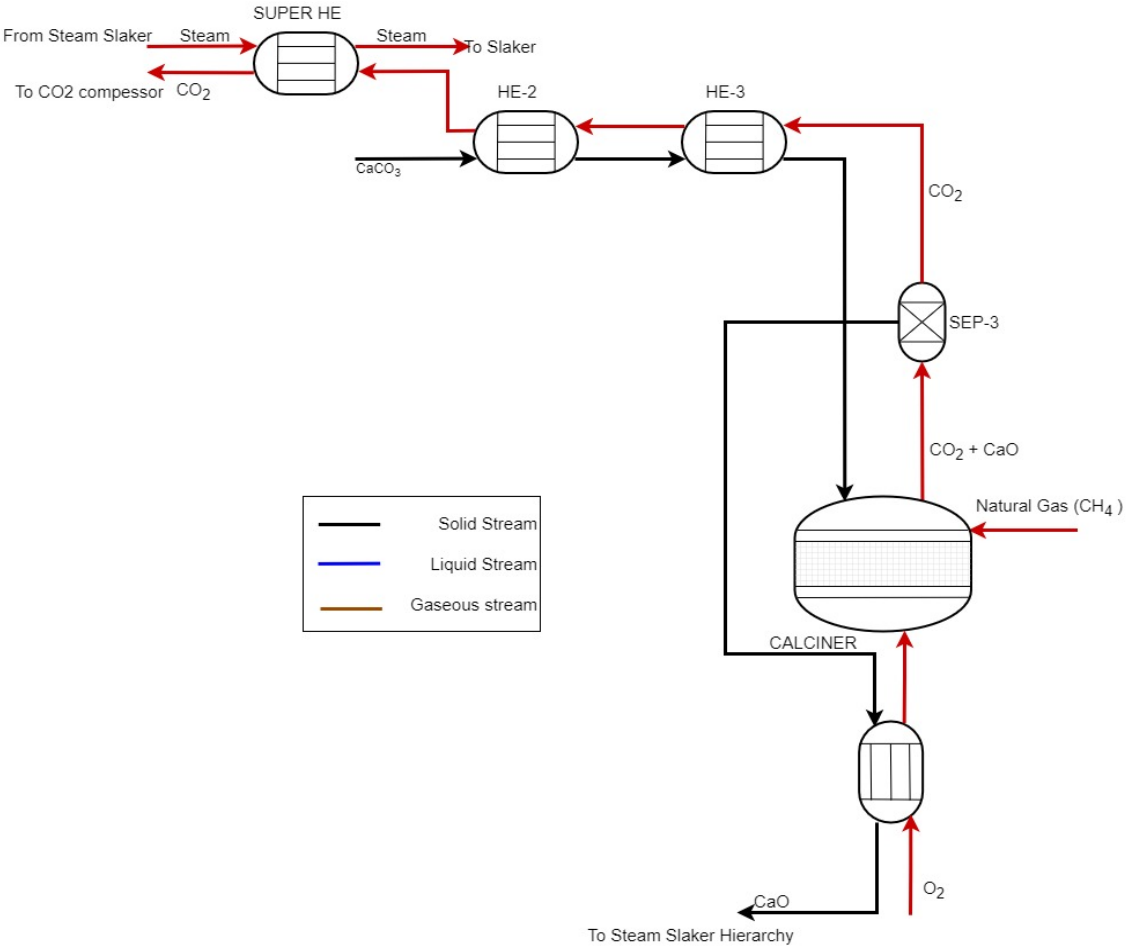

Figure 4.5: Calciner hierarchy [15]

4.1.1.5 Compressor

The CO_2 produced in the calciner is fed into a multistage compressor for sequestration. However, CO_2 mass fraction is still not sufficient to be directly considered for further sequestration. Therefore, before entering the compressor, it is "cleaned up" in a water knockout. It is a simple separator block where the CO_2 from the calciner is made to come in contact with water to cool the gas and to condense the water content inside it. By removing the water content in the off-gas from the calciner the CO_2 concentration is increased. The separator has been modelled in a way that it only sends gaseous compounds into the compressor and all the separated water is fed to the wash-tank in the slaker hierarchy.

The concentrated CO_2 is compressed from atmospheric to 15 MPa at 45°C as indicated by Keith et.al.[12]. This is done using a multi-stage compressor. The compressor undergoes four stages of compression which can be seen in **Figure 4.6** there are four compressors CMP1, CMP2, CMP3 and finally CMP4. The stages modelled all have the same pressure ratio of 3.5 in order to obtain a flow of concentrated CO_2 at 150 bar. The compressors used in the model are isentropic which have the same isentropic and mechanical efficiencies. All compressors used are considered as isentropic since no external heat is being added or extracted during the compression. Coolers have been used in the model as intercoolers. The intercoolers are isobaric with no pressure drop during cooling process and it aims to bring back the temperature to 45°C after each compression stage. The reason for intercooling is to reduce the compressor work as the temperature of gas can reach very high levels when the gas undergoes high levels of compression.

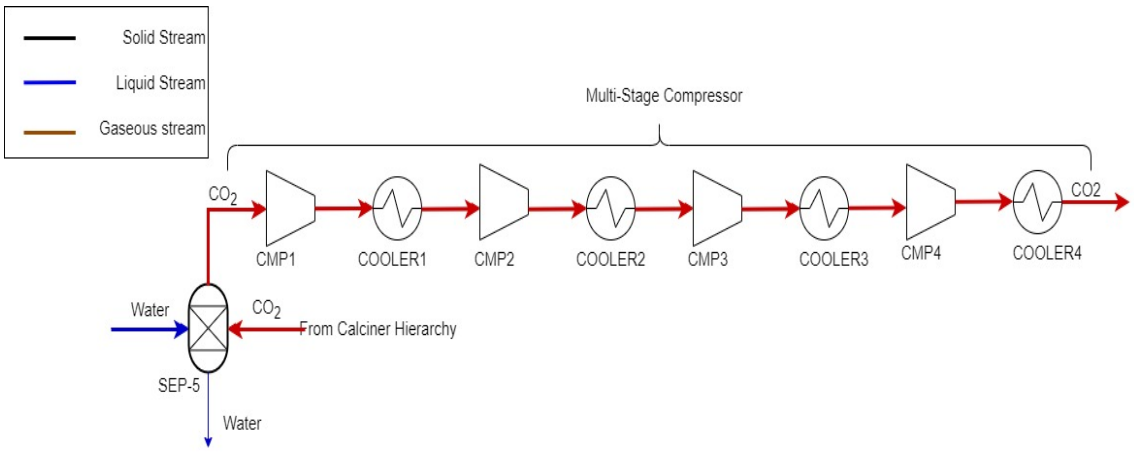

Figure 4.6: Compressor hierarchy [15]

4.2 Adsorbtion process

4.2.1 Modelling

The objective is to model the adsorption bed. This model is validated against the reference model[21]. Once validation is completed, the model is used as a tool for sensitivity analysis. The Adsorption model starts by the flue gas entering the adsorption bed also called the adsorption phase. This is done with the help of pressure increase created by a blower. A linear valve is used after the blower to control the flow of the input flue gas. Then the flue gas is passed through the adsorption bed which consists of solid sorbent Lewatit®VP OC 1065. The sorbent adsorbs CO_2 and H_2O from the flue gas. CO_2 adsorption follows Co-adsorption Toth isotherm and H_2O adsorption follows GAB isotherm model.

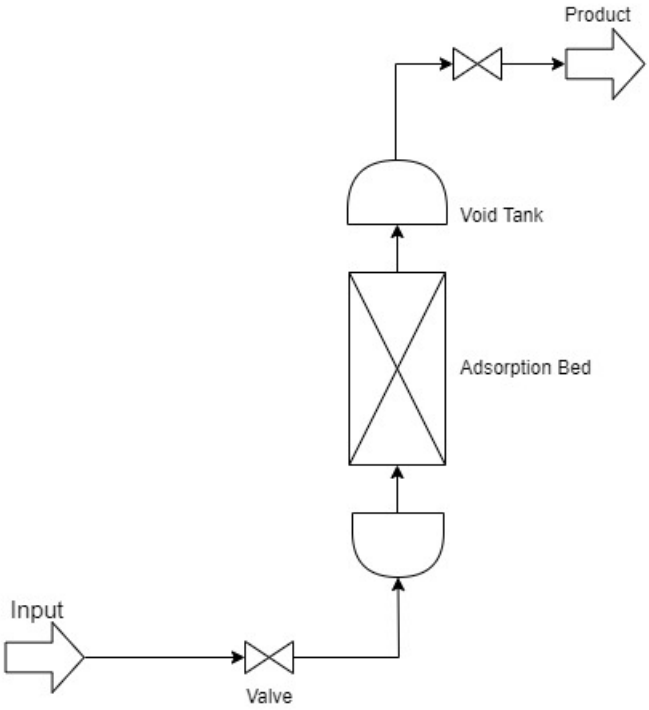

Figure 4.7: Adsorption model

4.2.1.1 Adsorption bed

Adsorption bed consists of solid sorbent Lewatit®VP OC 1065. In ASPEN adsorption co-adsorption toth isotherm model for CO_2 adsorption and GAB isotherm model for H_2O adsorption are not present in the inbuilt isotherms. Hence, the isotherms has to be coded into the model. There are two option for doing this. First one is to create a FORTRAN code and feed it in the user FORTRAN subroutine. The second method is to code the flowsheet constraints in system's modeling language. This thesis used the second option. Both isotherm models are a function of flue gas temperature and pressure. The flowchart of the isotherm model can be seen in **Figure 4.8**. All the parameters required for the isotherms to run were referred in [21]. The temperature dependent Toth isotherm parameters are presented in **table 4.2**.

Parameter	Value	Unit
T_o	298.15	K
$q_{\infty,0}$	4.86	$molkg^{-1}$
χ	0.0	_____
b_0	2.85×10^{-21}	Pa^{-1}
$-\Delta H_0$	117798	$Jmol^{-1}$
τ_0	0.209	_____
α	0.523	_____
γ	-0.137	_____
β	5.612	_____

Table 4.2: Co-adsorption Toth isotherm parameters [21]

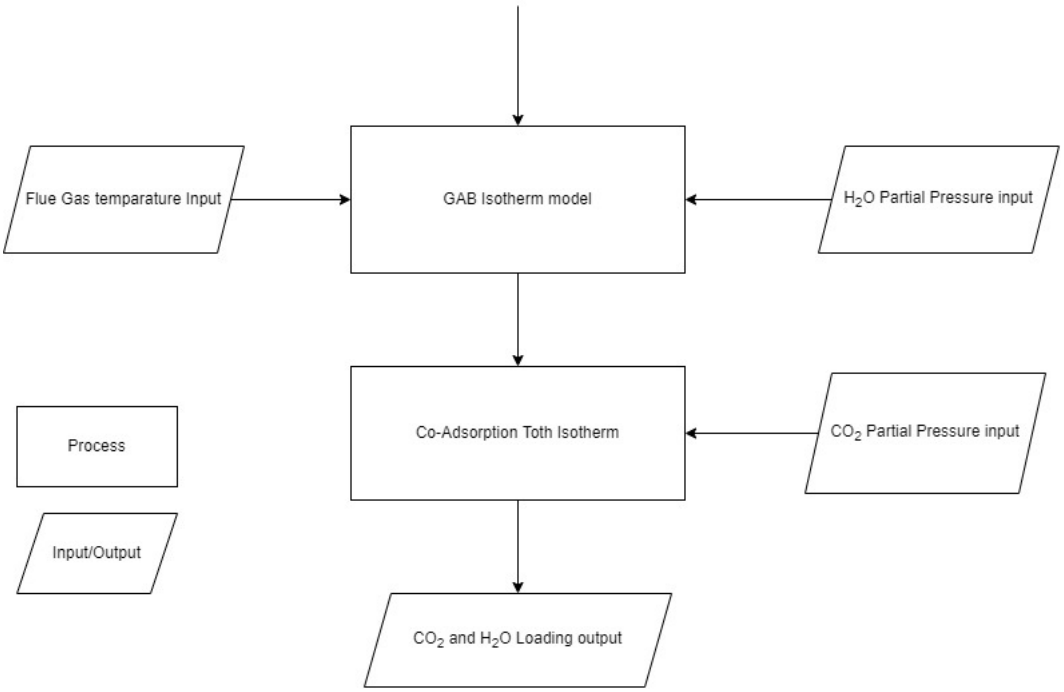

Figure 4.8: Isotherm modelling

The parameters used by temperature dependent GAB isotherm for H_2O adsorption is presented in **Table 4.3**.

Parameter	Value	Unit
q_m	3.63	$molkg^{-1}$
C	47110	$Jmol^{-1}$
D	0.023744	K^{-1}
F	57706	$Jmol^{-1}$
G	-47.814	$Jmol^{-1}k^{-1}$

Table 4.3: GAB isotherm parameters [21]

Parameter	Value	Unit
MTC_{CO_2}	0.003	s^{-1}
MTC_{H_2O}	0.0086	s^{-1}
DH_{CO_2}	-70000	$Jmol^{-1}$
DH_{H_2O}	-46000	$Jmol^{-1}$

Table 4.4: Kinetic model and energy model parameters [21]

The next step is to fill the adsorption bed block's configuration using parameters referred by John Young et.al.[21]. First is the general configuration of partial differential equation used for handling the model. The discretization method used in this model is upwind differencing scheme 1. This is the most common and preferred option because it is:

- Good all-round performer
- Unconditionally non-oscillatory
- Unconditionally stable
- Cheapest user of simulation time
- Reasonably accurate

The accuracy increases with increase in the number of axial nodes along the adsorption bed. Upwind Differencing scheme 1 is a first-order upwind differencing scheme, based on a first-order Taylor expansion which is shown in **Equation 2.20** of theory section. The number of nodes for the model is kept at 20.

Next is the material/momentum balance sheet where the assumption is that there is only convection for material balance [21].Ergun equation (**Equation 2.23** is used to model momentum balance.

Kinetics is modelled using lumped resistance model which takes a linear form. This means the mass transfer driving force for a component is a linear function of gas phase concentration (fluid film). More information can be seen in theory section **Equation 2.22**. The mass transfer coefficient of the components can be seen in **Table 4.4**. Coming to energy balance assumptions, it is assumed that there is non-isothermal with no conduction. This option ignores the axial thermal conduction for the gas and the solid phase. The heat of adsorption values for CO_2 and H_2O is shown in **Table 4.4**. Finally, specification of bed geometry, sorbent characteristics and feed conditions for Lewatit®VP OC 1065 is taken from [21] and is presented in **Table 4.5**.

4.2.1.2 Auxiliary units

The auxiliary units used are blower, vacuum pump and heater water pump. In the model linear gas valves with varying the Linear valve constants are used to depict both blower and vacuum pump. as per the pressure and flow requirement of each phase. Vacuum pump is used to create an under pressure environment (0.2 bar) in the adsorption bed for desorption of CO_2 and H_2O. For increasing the temperature in the adsorption bed, a heating jacket is used to increase the temperature to desorption temperature (353.15K-393.15K). the blower power and vacuum pump energy consumption is calculated using **Equation 2.23** and **Equation 2.23**. The specific

Parameter	Value	Unit
Mass-based adsorbent heat capacity $C_{p,s}$	1580	$Jkg^{-1}K^{-1}$
Particle radius R_p	0.26	mm
Bulk Density ϱ_b	630	kg m^{-3}
Bed Length L	0.01	m
Bed Diameter	0.1	m
Column constant for heat transfer coefficient	14	$W\ m^{-2}K^{-1}$
Feed Velocity v_{feed}	0.0706	ms^{-1}
feed temperature T	288.15	K
Feed relative humidity RH	0.55	____
feed CO_2 concentration	0.04	%
feed pressure	1.1013	bar

Table 4.5: Adsorbent, column and feed condition parameters [21]

power of the pump is given by **Equation 2.25**. The efficiencies of the pumps and blowers is given in **Table 4.6**.

Parameter	Value	Unit
η_{blower}	0.7	____
η_{vac}	0.5	____
η_{w}	0.7	____

Table 4.6: Auxiliary unit efficiency[21]

4.2.1.3 Cycle organiser

Once the single bed model is complete all the phases of the TVSA cycle (adsorption, vacuum, heating, desorption, cooling and pressurization) need to be depicted where each of the phases is time driven. Cycle organiser component is used to depict this whole cycle. Time of each phase of a cycle is given in **table 4.7** [21].

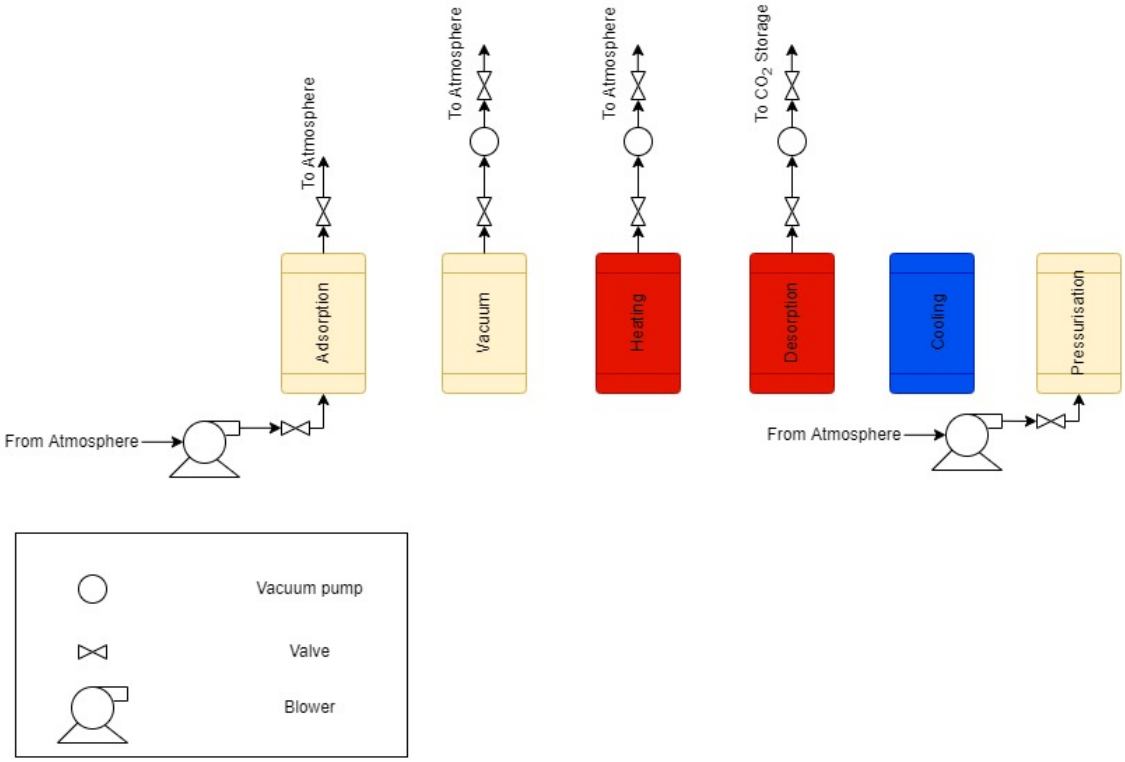

Figure 4.9: Cycle organiser[21]

Phase	Time (s)
Adsorption	8500
Vacuum	100
Heating	100
Desorption	18000
Cooling	100
Pressurization	100

Table 4.7: Cycle organiser time [21]

5

Model validation

5.1 Absorption process

The absorber column in model was validated by comparing the CO_2 loading and CO_2 capture rate with the reference [13], which uses 100% CO_2 flue gas (there was no research work found with experimental loading of CO_2 on KOH solution at air concentration). Once the concentration was set, CO_2 loading and capture rate at different KOH solution concentration, temperature and pressure were calculated as: reference[13]. Capture rate and CO_2 loading were calculated using the **Equation 5.1** and **Equation 5.2** respectively.

$$CO_2\text{Capturerate} = \frac{[CO_2]\text{outlet}}{[CO_2]\text{inlet}} \tag{5.1}$$

$$CO_2\text{Loading} = \frac{[HCO_3^-] + [CO_3^{2-}]}{[K^+]} \tag{5.2}$$

In **Equation 5.1** $[CO_2]$outlet is the mole flow of CO_2 in the exhaust of the absorber column and $[CO_2]$inlet is the mole flow of CO_2 in the inlet flue gas of the absorber column. In **equation 5.2** $[HCO_3^-]$ is the mole flow of Bicarbonate ion in the loaded K_2CO_3 solution coming out of the absorber column. $[CO_3^{2-}]$ is the mole flow of carbonate ion the loaded K_2CO_3 solution coming out of the absorber column, and finally $[K^+]$ is the mole flow of the potassium ion in the loaded K_2CO_3 solution coming out of the absorber column.
The results of absorber column validation can be seen in **Figure 5.1** and **Figure 5.2**.

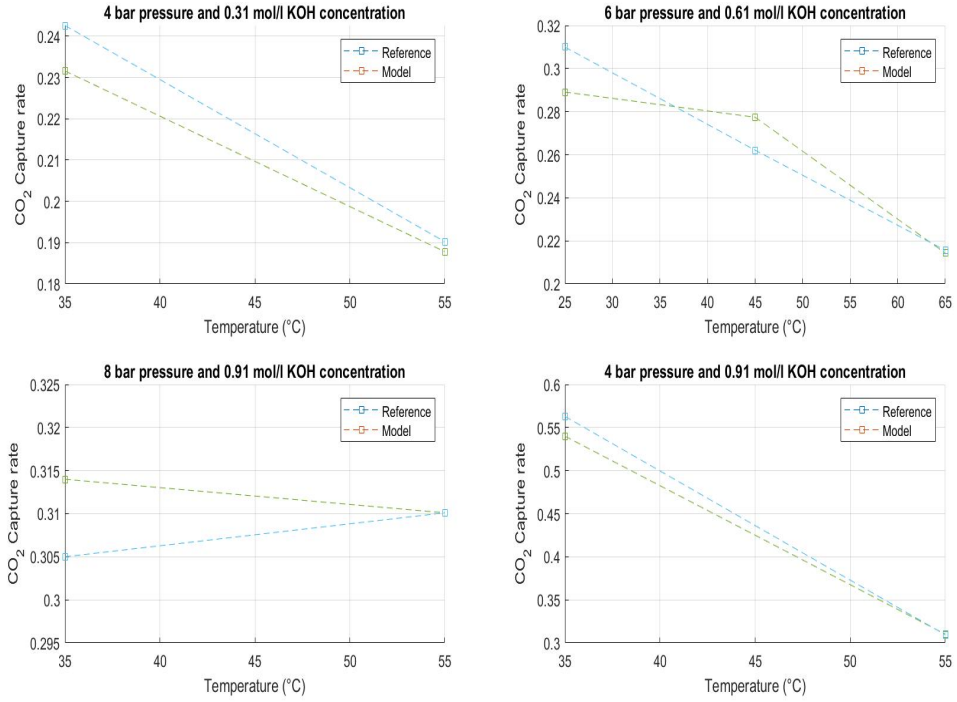

Figure 5.1: CO_2 Capture rate in absorber column using KOH solution

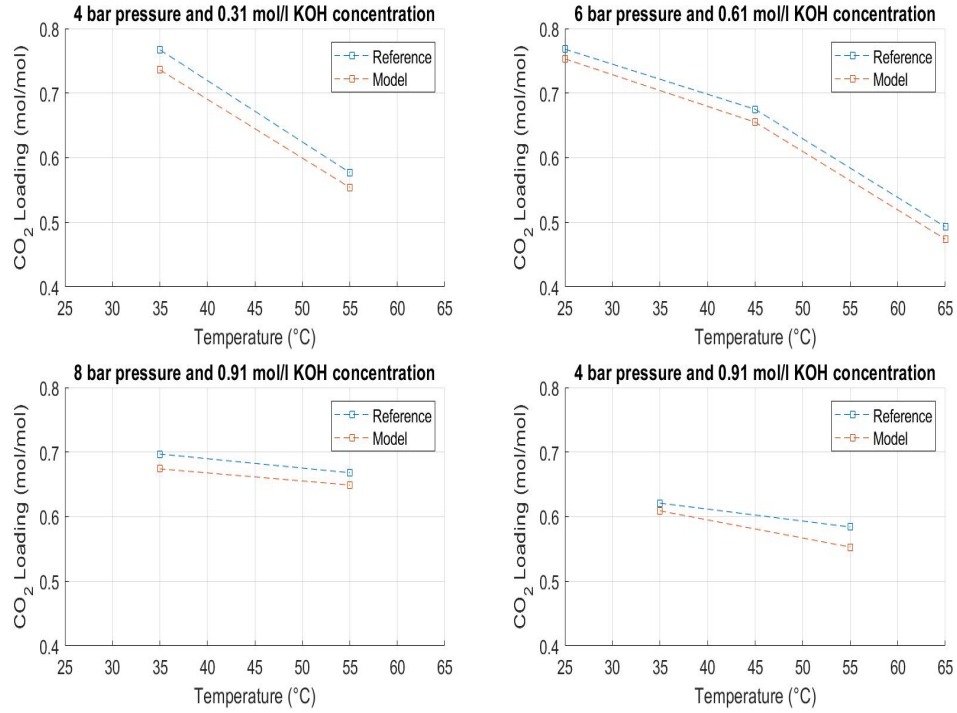

Figure 5.2: CO_2 loading on KOH solution

From **Figure 5.1** and **Figure 5.2** it can be seen that the average deviation of model's loading and capture rate when compared to [13] is 3.079% and 3.165% respectively.

Total energy consumption by the model and reference [12] were compared. First the electricity consumed was compared (see**Table 5.1**).

Components	**Keith et.al. (kWh/tCO2)**	**Model (kWh/tCO_2)**	**Source**
Air Contactor	62.162	811.330	Modeled
Pellet Reactor	23	27.64 0	Modeled
Slaker	24.201	24.201	Reference[12]
Calciner	5.378	5.378	Reference[12]
Quicklime Tank	1.344	1.344	Reference[12]
Wash Tank	2.016	2.016	Reference[12]
ASU	89.412	89.450	Model
AUX	17.479	17.479	Reference[12]
CO_2 Compressor	147.9	120.950	Model

Table 5.1: Electricity consumption

The electricity consumption in both model and reference [12] can be better envisioned from **Figure 5.3** and **Figure 5.4** respectively. From the figures it can be seen that the unit that is consuming the most electricity in our modeled case is the absorber air blower(around 811.33 kWh/tCO_2).

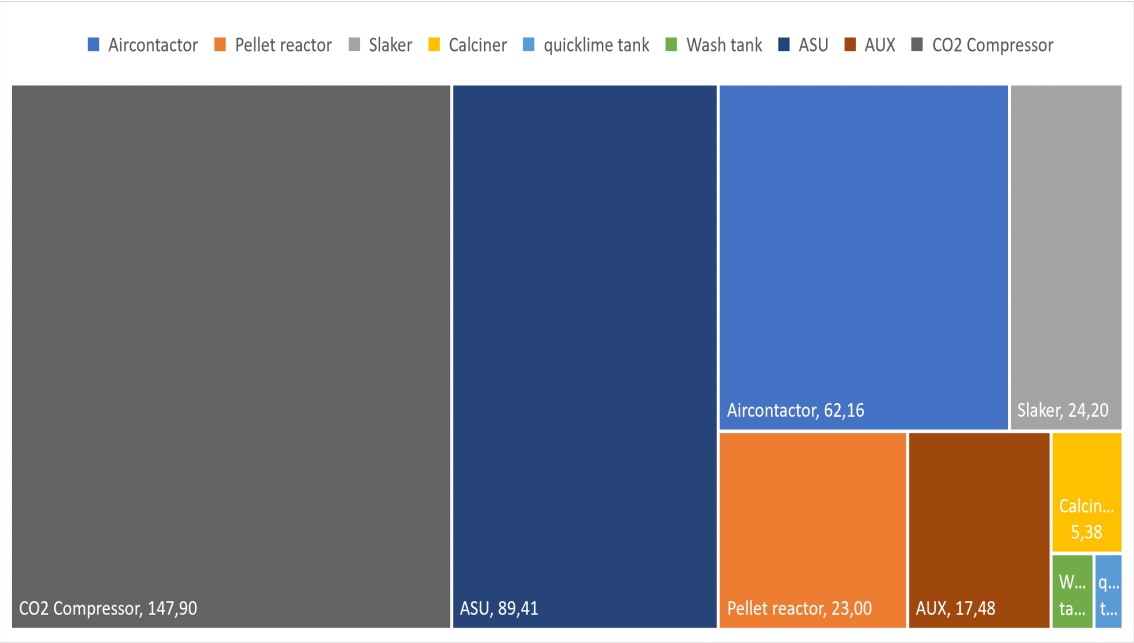

Figure 5.3: Electricity consumed in reference case[12].

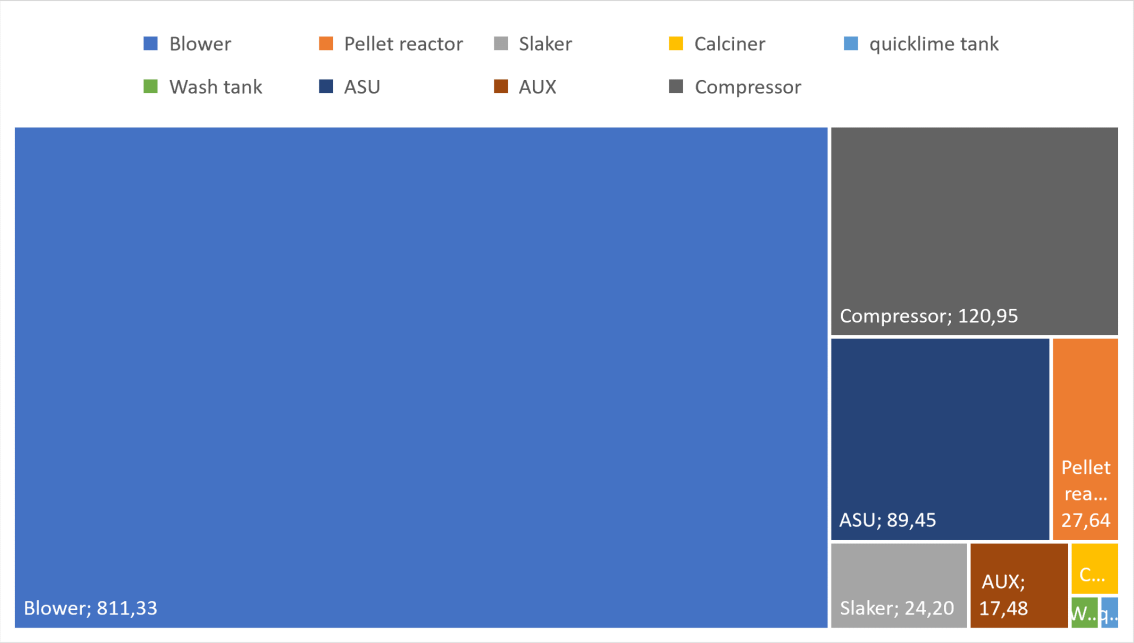

Figure 5.4: Electricity consumed in our modeled case

The problem with **Figure 5.3** and **Figure 5.4** was that the model's blower consumption was overpowering all other consumption. From **Figure 5.5** and **Figure 5.6** which shows the combined consumption of both natural gas and electricity requirement in GJ/tCO_2 of both model and reference [12] in two different cases which are with blower consumption and without blower consumption to get a better idea of energy consumption comparison.

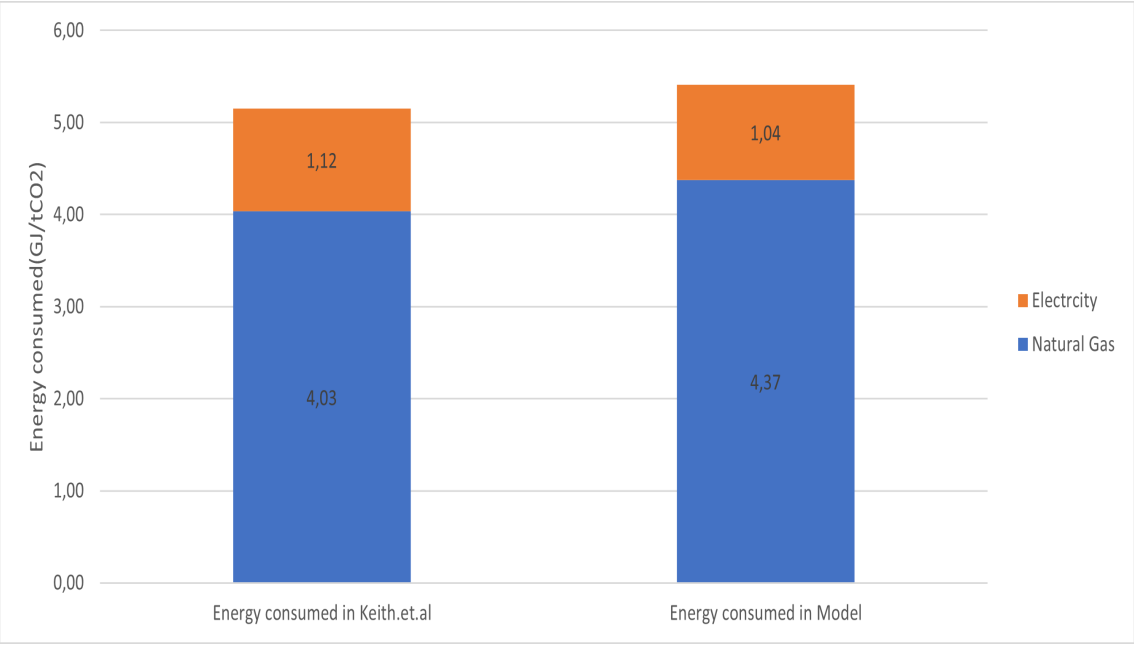

Figure 5.5: Energy consumed (without blower consumption)

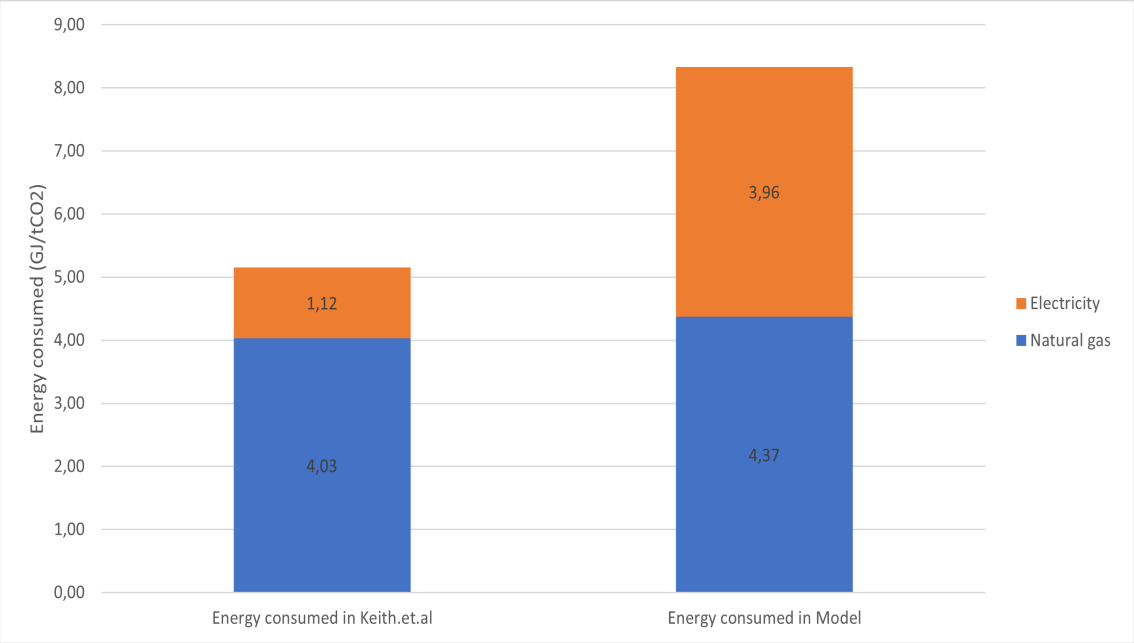

Figure 5.6: Energy consumed (with blower consumption)

From **Figure 5.5** we can see that if we exclude blower and air contactor electricity consumption the difference between model and reference total energy consumption is 4.794%. Difference in specific energy consumption when comparing with and without blower is because of the very high specific energy consumption of blower which also means that the absorber column works on a very low scale when compared to air contactor.

5.2 Adsorption process

The co-adsorption Toth model and GAB model that were programmed are validated by comparing the model's loading [$kmol_{CO_2}/g$] of CO_2 and H_2O to the experimental loading values of the reference[21]. Initially the isotherm model was validated in steady state. To validate the loading of the model against that of the reference, the adsorption bed sizing, feed values and material specifications were replicated with parameters shown in **Table 4.5** and the results can be seen in **Figure 5.7** and **Figure 5.8**.

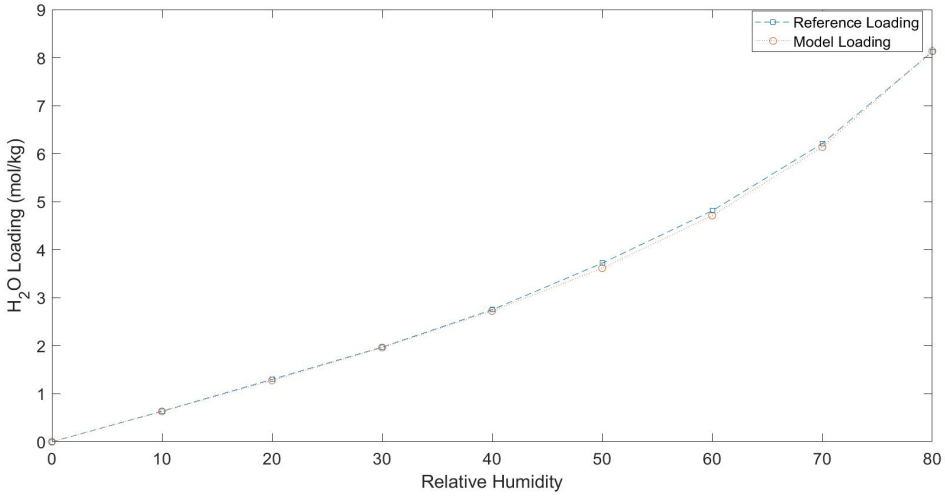

Figure 5.7: H_2O Loading

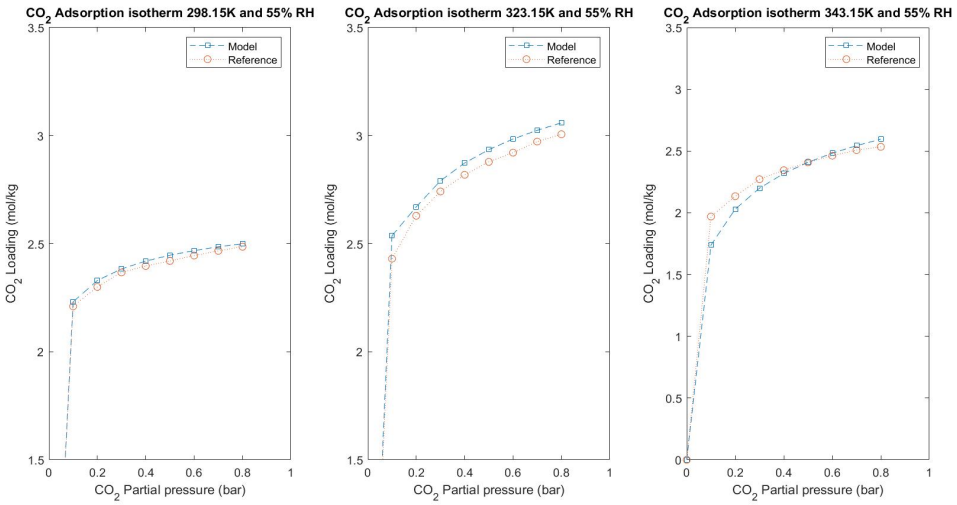

Figure 5.8: CO_2 Loading

When validating H_2O loading the relative humidity in the input flue gas is varied to see the how it effects the loading and validate the trend of variation keeping temperature constant. Slight differences in loading values observed from the model and the reference values are due to heat losses in the experimental values which are not

taken into consideration in the model as it is adiabatic[21]. When validating CO_2 loading the partial pressure of the same is varied along with the flue gas temperature to see if the loading follows the same trend as the reference values.

Validation of the dynamics was done by comparing the breakthrough curve of the model against that of the reference; see the validation of breakthrough curve for both co-adsorption Toth isotherm and GAB isotherm in **Figure 5.9** and **Figure 5.10**.

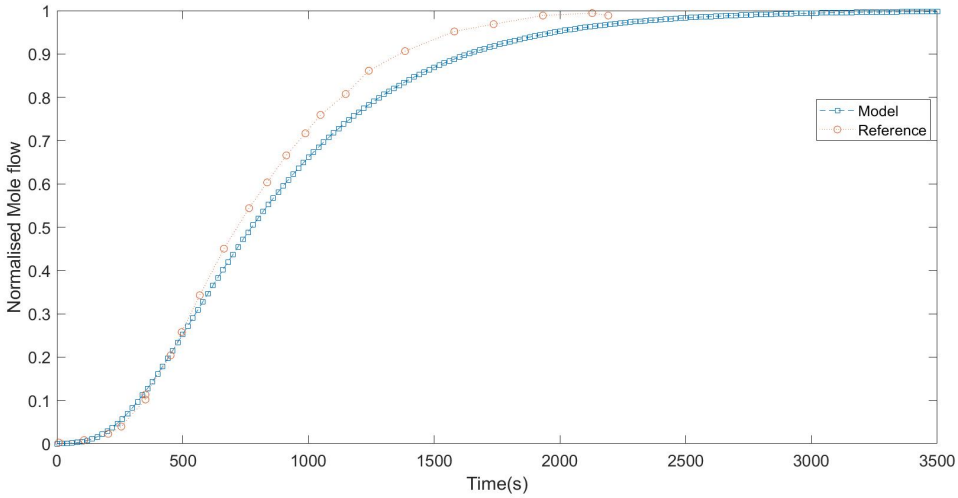

Figure 5.9: CO_2 breakthrough curve at 75C and 0% RH[21]

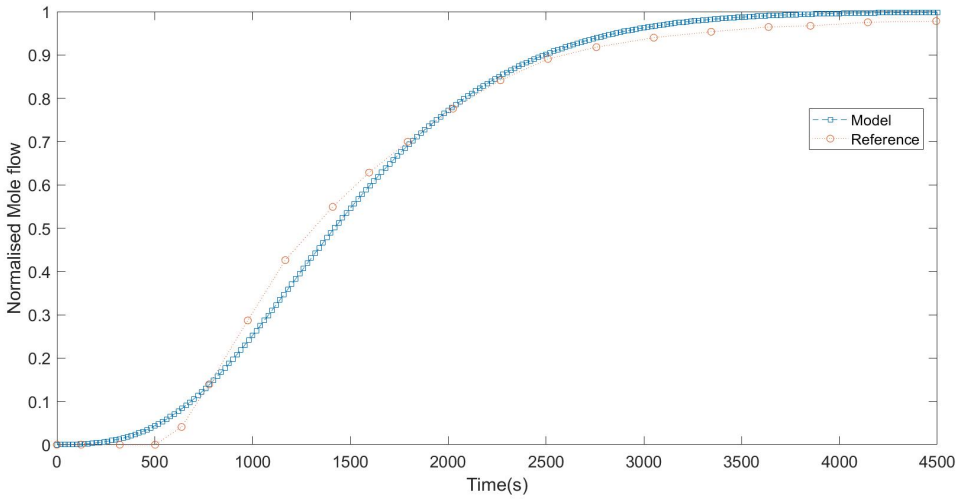

Figure 5.10: H_2O breakthrough curve at 25C and 30% RH[21]

From **Figure 5.9** and **Figure 5.10** it can be seen that there is slight difference between the model's breakthrough curve and the reference's. It is again due to the thermal losses in the reference experimental setup[21].

Validation of the VTSA was done by comparing the breakthrough curve of the CO_2 concentration in the exhaust, dynamic Temperature curve, CO_2 loading curve of CO_2 and the dynamic pressure curve with that of the reference [21]. The cycle organiser was set using the time values as shown in **Table 4.7**.

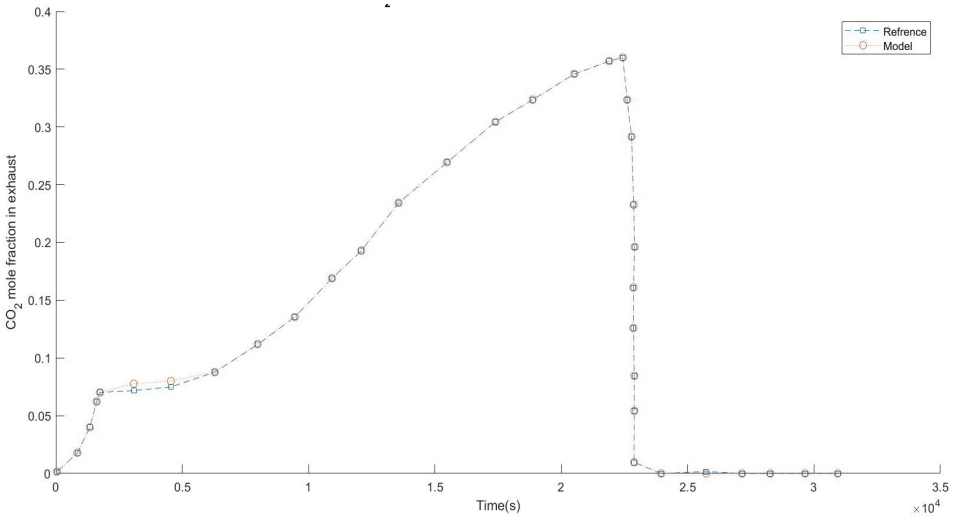

Figure 5.11: CO_2 mole fraction curve [21]

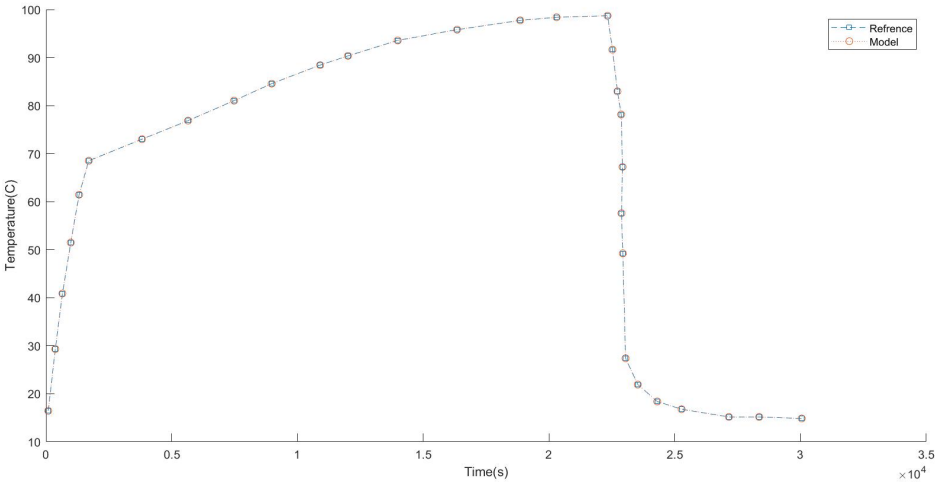

Figure 5.12: Dynamic temperature curve [21]

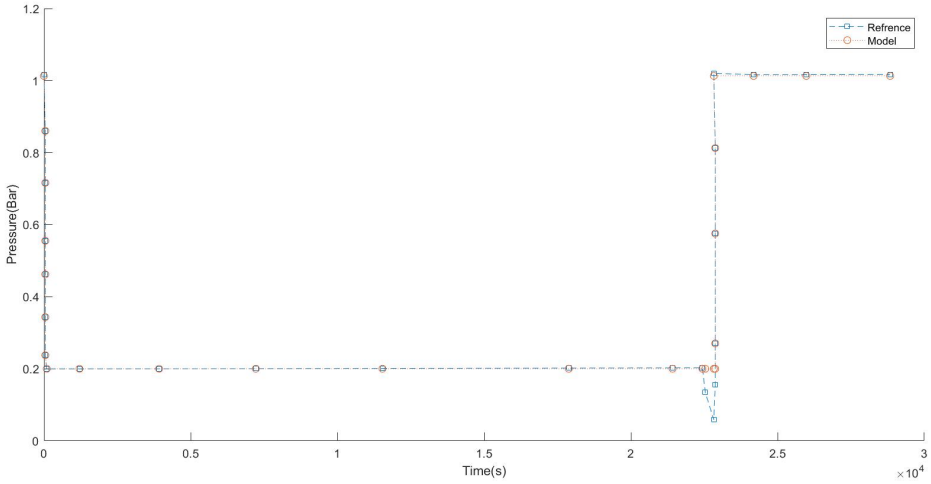

Figure 5.13: Dynamic pressure curve [21]

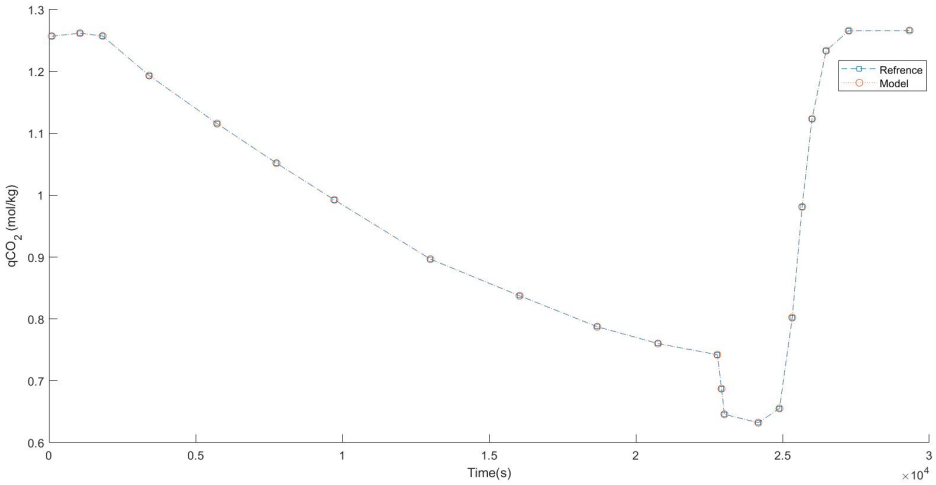

Figure 5.14: Dynamic loading curve [21]

textbfFigure 5.11 shows the CO_2 mole fraction in the adsorption bed exit. From 23001-31000s the bed is in adsorption phase. From 1-200s both vacuum phase and heating phase occurs. From 201s to 22800s desorption process takes place. Finally, from 22800-23000s Cooling and pressurization phase takes place which completes 1 cycle of VTSA. **Figure 5.12** shows the temperature of flue gas in the adsorption bed exit. **Figure 5.13** shows the pressure at the end of adsorption bed. **Figure 5.14** shows the dynamic loading of CO_2 on Lewatit®VP OC 1065 at the 10th node of the adsorption bed.

Finally the work equivalent of the whole VTSA cycle was validated - see **Table 5.2**. The total work equivalent value for the model was compared with the reference value (textbfFigure 5.15), yielding a deviation to the reference's value of 1.28%.

Parameter	Value	Unit
W_{vac}	1.157	$MJkg^{-1}_{CO_2}$
W_{blower}	0.924	$MJkg^{-1}_{CO_2}$
W_{pump}	0.021	$MJkg^{-1}_{CO_2}$
Heat jacket work	1.750	$MJkg^{-1}_{CO_2}$
Total W_{eq}	3.850	$MJkg^{-1}_{CO_2}$

Table 5.2: Work Equivalent of Model

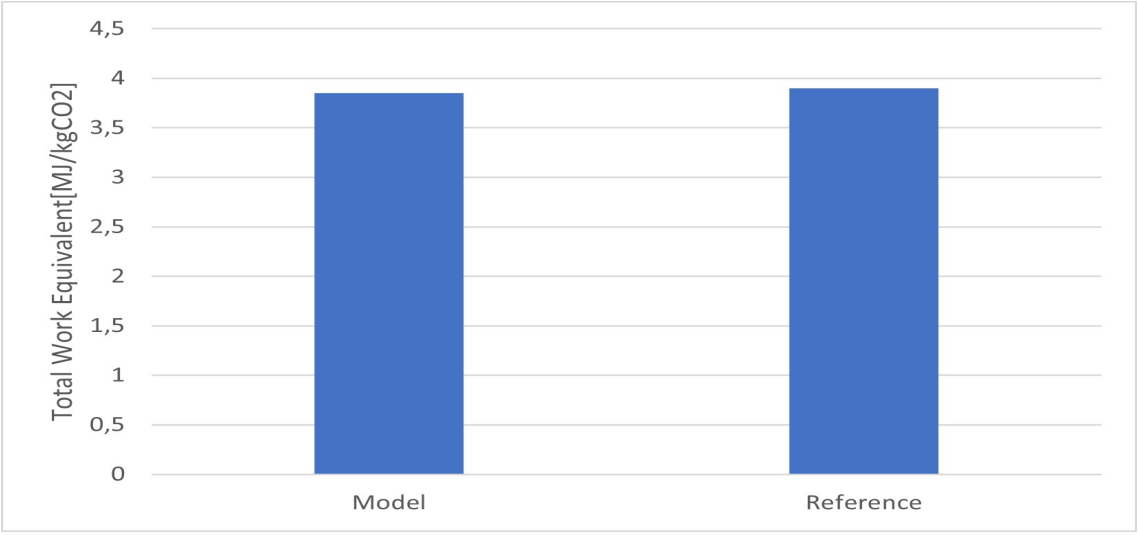

Figure 5.15: Work Equivalent comparison

6

Results & Discussion

6.1 Absorption process

6.1.1 Sensitivity on flue gas mass flow rate

In this case of sensitivity analysis both CO_2 concentration and CO_2 capture rate were kept at the base case values and the flow rate of the flue gas was changed from very small flow rate of 30t/h to 140t/h. (140t/h is maximum calculated flow rate of flue gas in the manufacturing plant). The specific energy consumed with varying mass flow rate of flue gas can be seen in **Figure 6.1**.

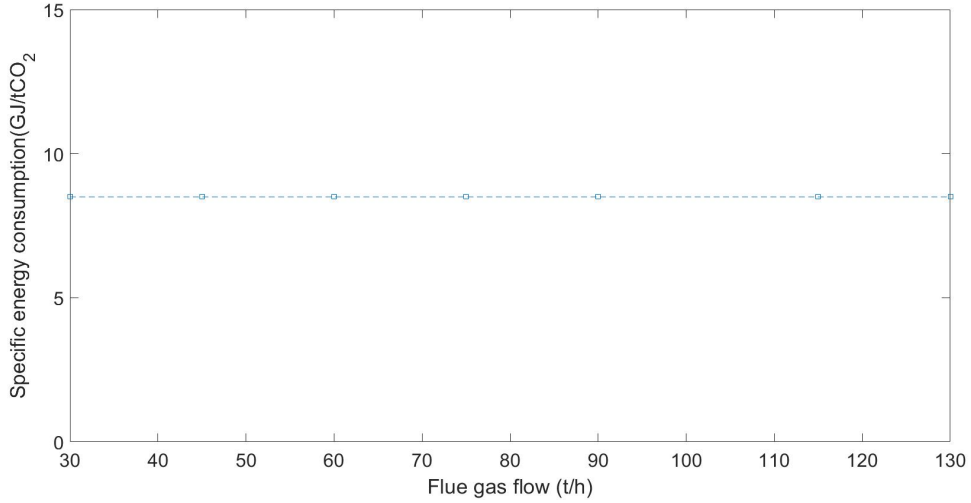

Figure 6.1: Specific energy consumed varying flue gas mass flow rate

From **figure 6.1** we can see that varying the flue gas mass flow rate has no effect on the specific energy required. This is because change in flow rate give a proportional change in all the other parameters in the model including the CO_2 captured, which results in a constant specific energy consumed.

6.1.2 Sensitivity on capture rate

In this case both flue gas mass flow rate and CO_2 concentration were kept constant at the base case values and the CO_2 capture rate was varied from 10% to 90%. The

variation of specific energy consumed for varying CO_2 capture rate can be seen in **Figure 6.2**.

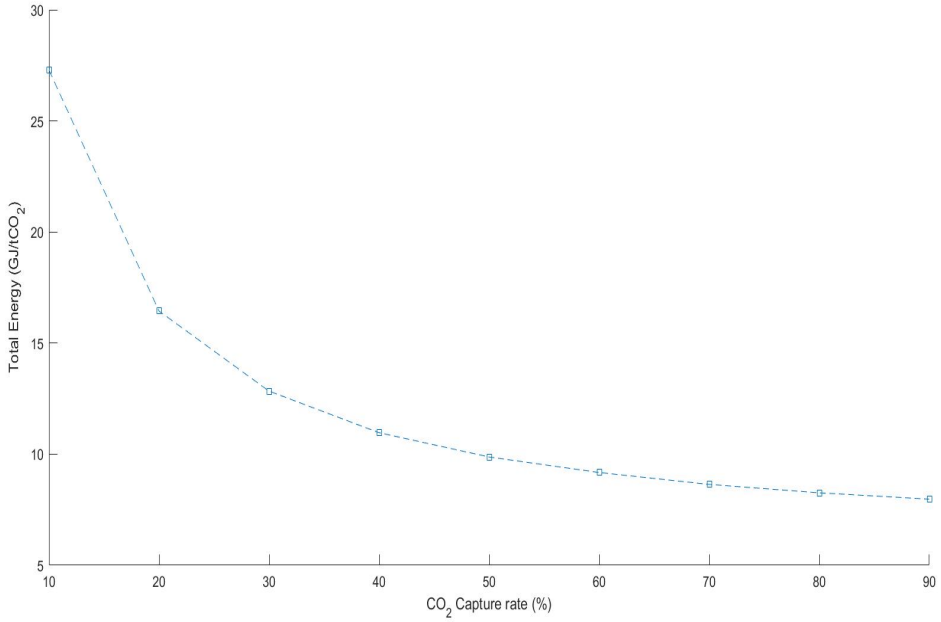

Figure 6.2: Specific energy consumed (varying capture rate)

From **figure 6.2** we can see that with increasing capture rate, specific energy consumption reduces exponentially. The reason for this is reduction in blower consumption. In order to verify **figure 6.3** was generated, this shows that blower consumption is mainly responsible for this reduction trend. In **figure 6.3** "rest consumption" are all other electricity consumers which can be seen in **table 5.1**. NG is the specific Natural gas being consumed in the calciner.

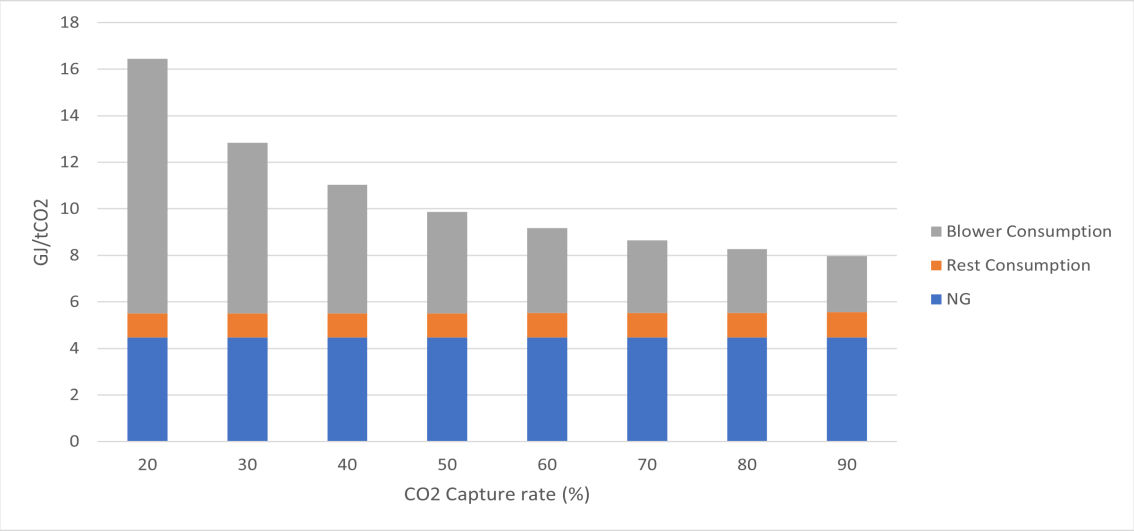

Figure 6.3: Specific energy consumed stacked bar graph (varying CO_2 capture rate)

Figure 6.4 shows that by excluding the blower's consumption, rest of the con-

sumers' consumption was slightly increasing. It was also seen that in the rest of the consumers, only the pellet reactor pump consumption was increasing and to see that clearly **Figure 6.5** was generated from which it is clear that the specific electricity consumption of pellet reactor pump is increasing with increase in capture rate.

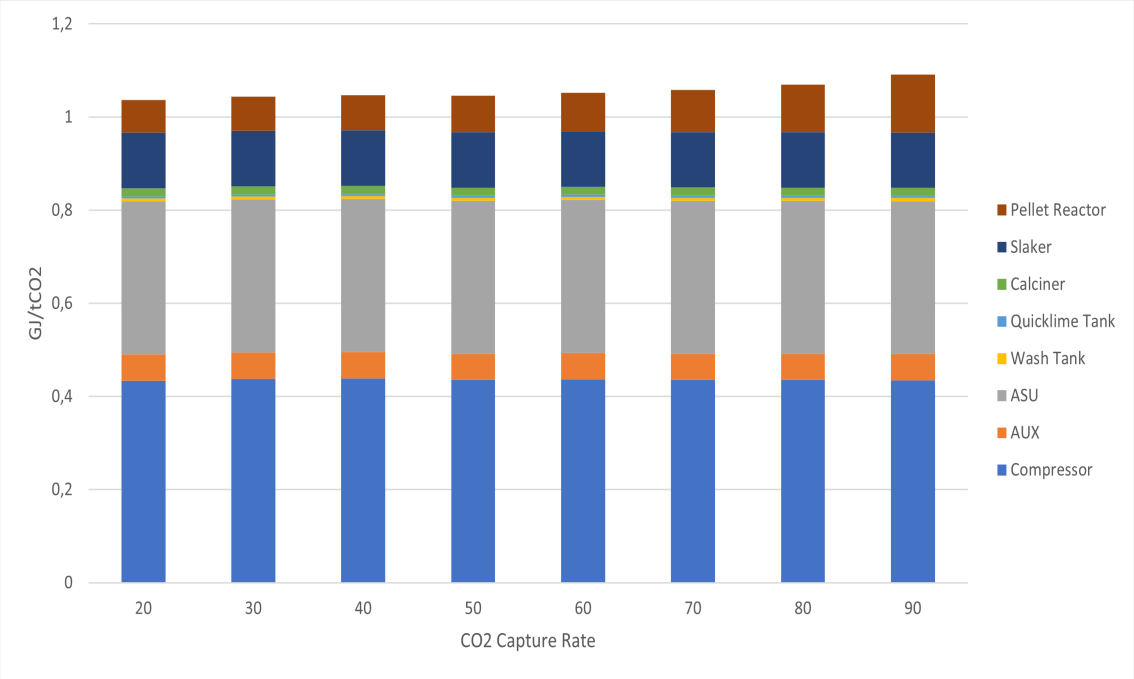

Figure 6.4: Electricity consumers stacked bar graph excluding blower (varying CO_2 capture rate)

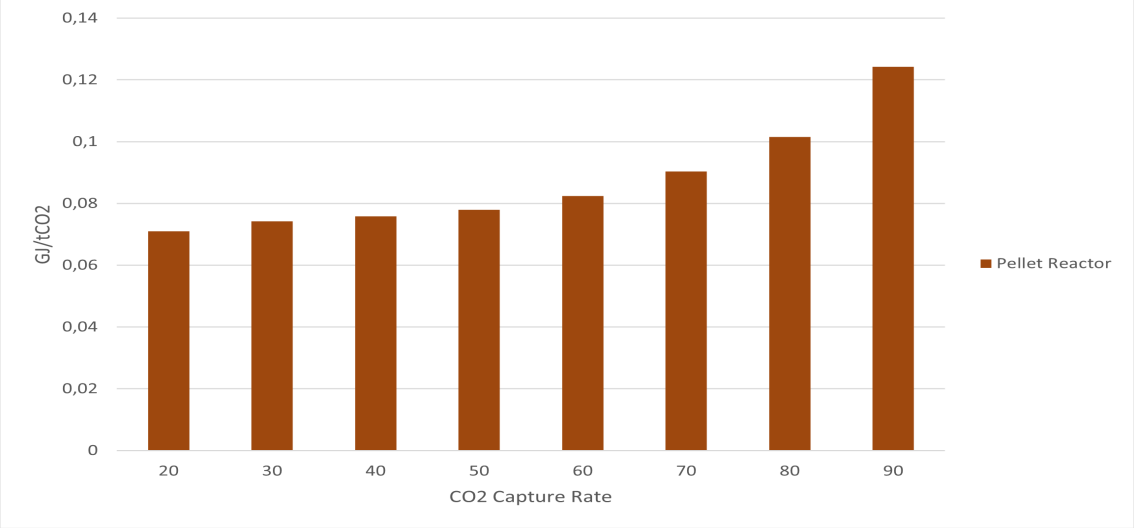

Figure 6.5: Pellet reactor specific electricity consumption(varying CO_2 capture rate)

6.1.3 Sensitivity on CO_2 concentration

With varying CO_2 concentration in flue gas, the specific energy consumed reduces at a very high rate until 1.5% concentration then it evens out. This is because of

sudden increase in amount of CO2 captured which is result of sudden decrease in the specific energy consumption of blower at the absorber column inlet. This rate of reduction becomes small when it reaches higher concentration as specific energy consumption of blower remains almost constant when concentration goes beyond 1.5% CO2 concentration

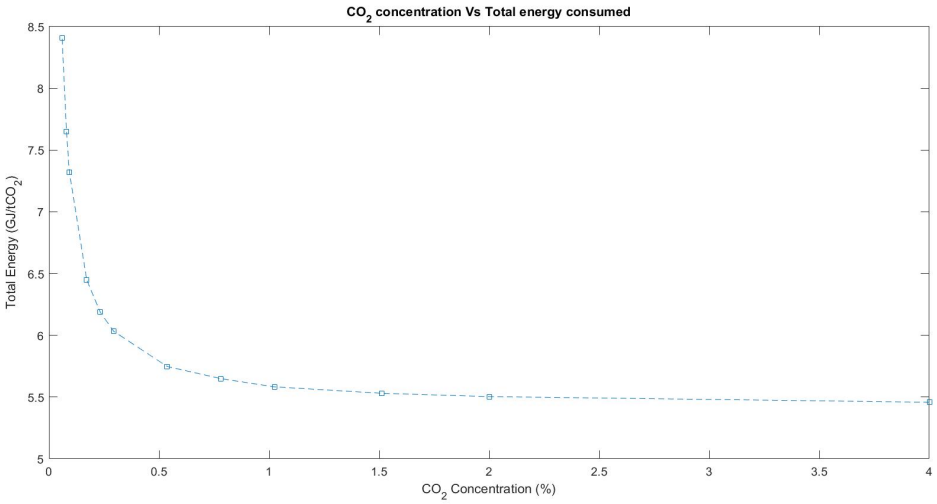

Figure 6.6: Specific energy consumption for varying CO_2 concentration

6.1.4 Summary

With sensitivity analysis completed, it was seen that capture rate less than 75% is not that interesting as the energy consumption is high when compared to conventional CCS technology.Hence, more cases were analysed on both varying CO_2 capture rate as well as varying CO_2 concentration but the capture rate was varied only over 75%. The resulting data was interpolated to **figure 6.7**.Contour plot can be seen in appendix.

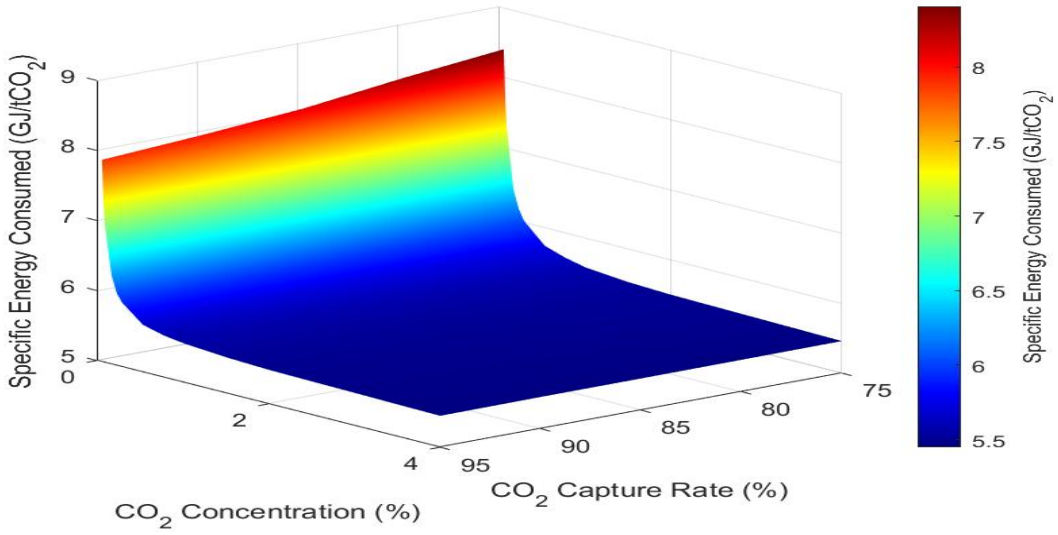

Figure 6.7: Surface plot with varying CO_2 capture rate and CO_2 concentration

6.2 Adsorption process

6.2.1 Sensitivity on column thickness

It can be seen from **figure 6.8** that with increasing column thickness the specific energy consumption reduces. This is mainly due to decreased specific blower and pump work which is a consequence of increasing CO_2 captured. The increase in the CO_2 captured is due to increasing sorbent material. The sudden reduction in specific energy consumption with increase in concentration is due to sudden decrease adsorption time and the amount of CO_2 adsorbed, which explains the reduction in specific heat required. The capture rate for all the three concentrations are almost the same due to constant CO_2 concentration at the exhaust(10%). This is so, because of adsorption process being an event driven process where the process stops as soon as the 10% CO_2 concentration is reached in the exhaust leading to a constant capture rate for all the cases even though the column thickness is varying as shown in **Figure 6.9**.

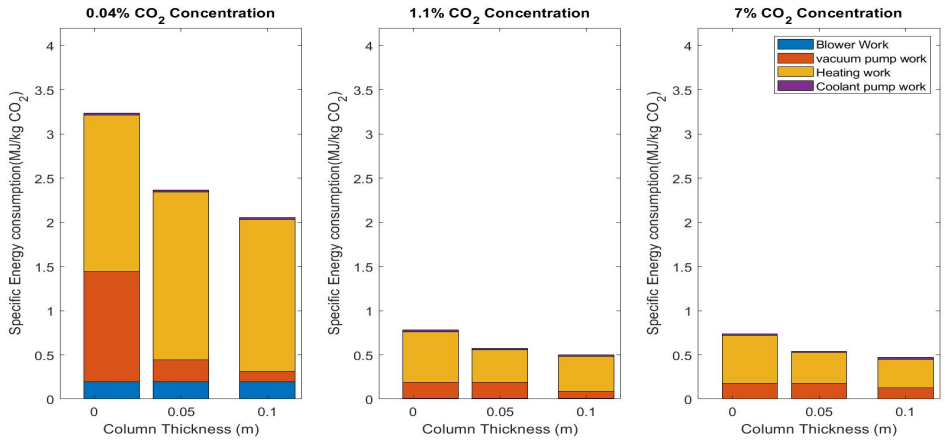

Figure 6.8: Specific energy consumed by model for varying column thickness

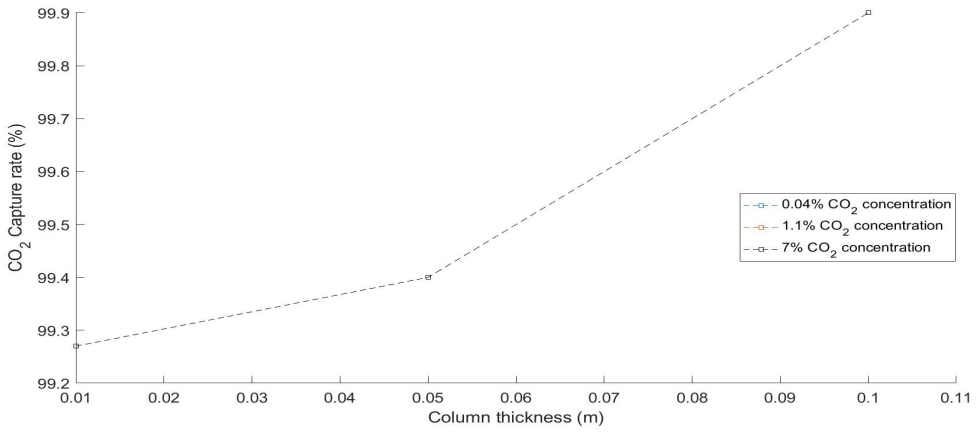

Figure 6.9: CO_2 capture rate of model for varying column thickness

6.2.2 Sensitivity on desorption temperature

It can be seen that with increasing desorption temperature the specific energy consumption increases at higher rate from 353.15K to 373.15K. But, is almost constant when the temperature is increased from 373.15K to 393.15K. This, since after a certain value of desorption temperature the increment in amount of heat required is offset by decreasing desorption time, as shown in **Figure 6.10**. The sudden reduction in specific energy consumption for 1.1% case is due to sudden decrease in adsorption time and the amount of CO_2 adsorbed, which explains the reduction in specific heat required. The blower work and the vacuum pump work are constant as the column thickness is constant. The capture rate for all the three concentrations are almost the same due to constant CO_2 concentration at the exhaust(10%). This is so, because of adsorption process being an event driven process where the process stops as soon as the 10% CO_2 concentration is reached in the exhaust leading to a constant capture rate for all the cases even though the column thickness is varying as shown in **Figure 6.11**.

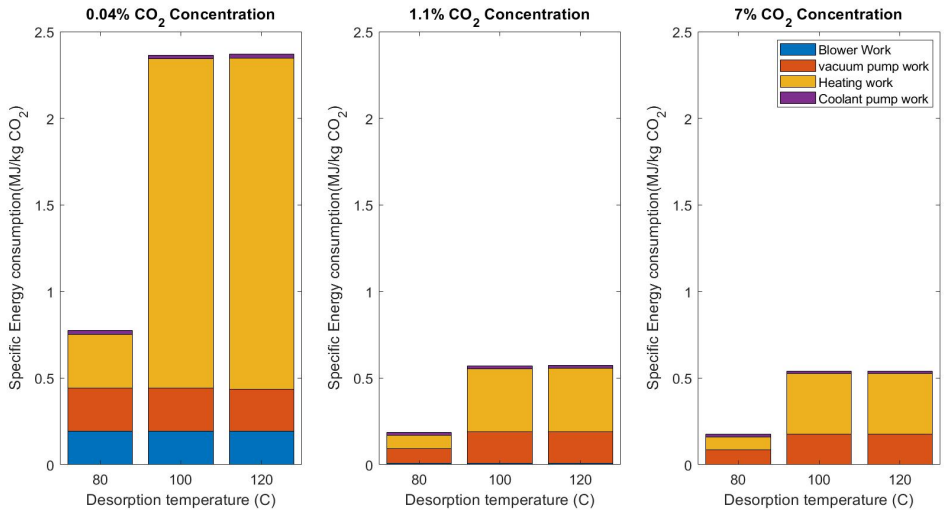

Figure 6.10: Specific energy consumed by model for varying desorption temperature

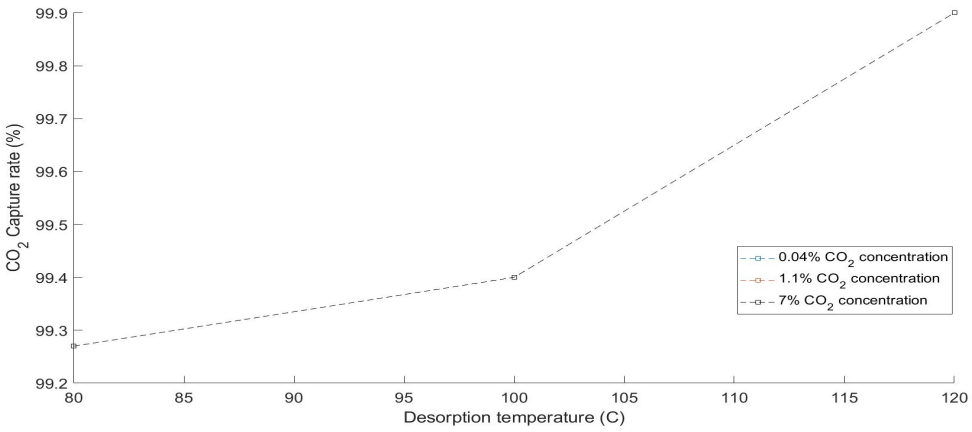

Figure 6.11: CO_2 capture rate of model for varying desorption temperature

6.2.3 Sensitivity on CO_2 concentration in exhaust

It can be seen that with increasing CO_2 concentration in exhaust the specific energy consumption (SEC) increases slightly 0.04% and 1.1% CO_2 concentration in flue gas but for 7% concentration there is an extreme reduction in capture rate leading to reduction in specific energy consumed . At lower concentration cases due to slight increase in blower work with very low increase in CO_2 captured leading to small increase in SEC. In this case the relation between capture rate and the specific energy consumed can be clearly seen.**Figure 6.16** and **Figure 6.17** show how the sudden reduction in specific energy consumption with increase in concentration is due to sudden decrease adsorption time and the amount of CO_2 adsorbed, which even explains the reduction in specific heat required as well. The blower work and the vacuum pump work is constant as the column thickness is constant.

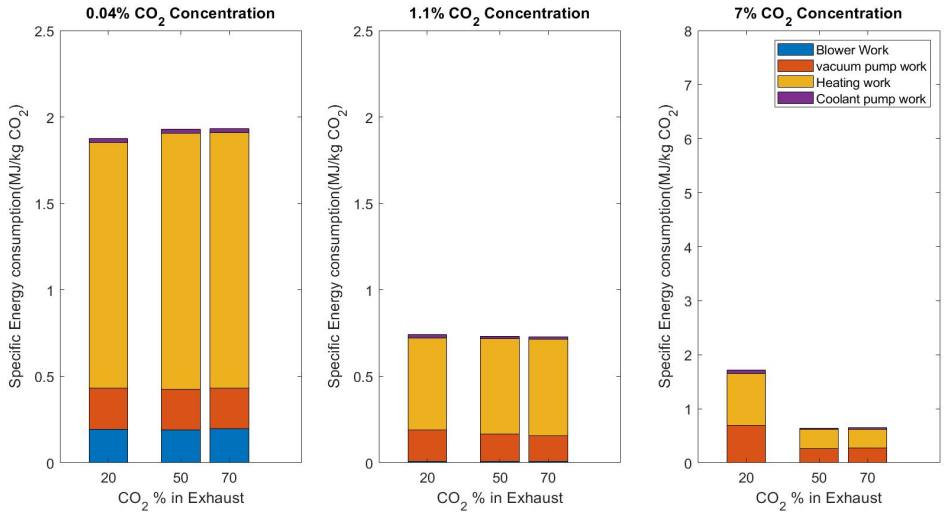

Figure 6.12: Specific energy consumed by model for varying CO_2 concentration in exhaust

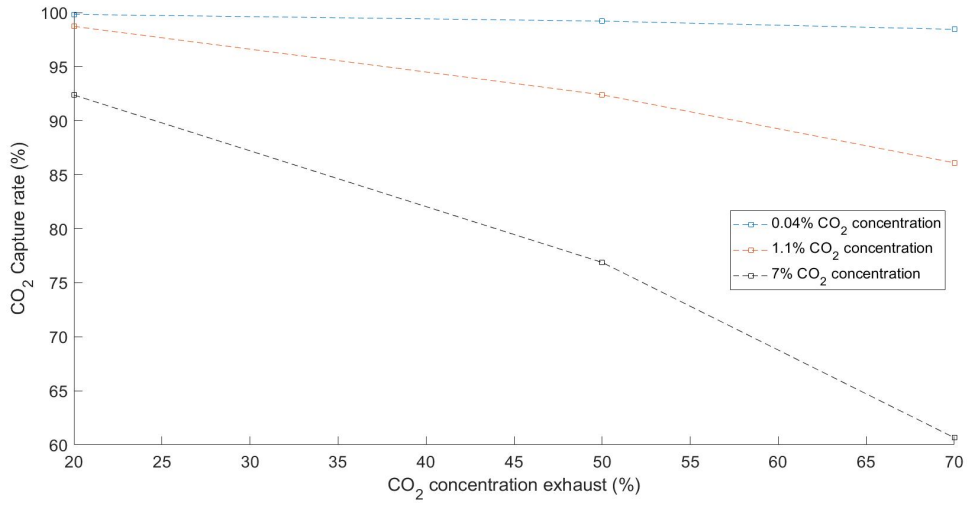

Figure 6.13: CO_2 capture rate of model for varying CO_2 concentration in exhaust

6.2.4 Sensitivity on superficial Velocity

It can be seen in **figure 6.14** that with increasing superficial velocity the specific energy consumption increases. This is due to increase in the specific blower energy consumption as the flue gas volumetric flow rate increases. The sudden reduction in specific energy consumption with increase in concentration is due to sudden decrease in adsorption time and the amount of CO_2 adsorbed due to variation in CO_2 loading, which even explains the reduction in specific heat required. The heating work and the vacuum pump work are constant as the column thickness is constant. This is so, because the heater and vacuum pump need to heat and reduce pressure respectively of a constant volume bed. The capture rate for all the three concentrations are almost the same due to constant CO_2 concentration at the exhaust(10%). This is so, because of adsorption process being an event driven process where the process stops as soon as the 10% CO_2 concentration is reached in the exhaust leading to a constant capture rate for all the cases even though the column thickness is varying as shown in**Figure 6.15**.

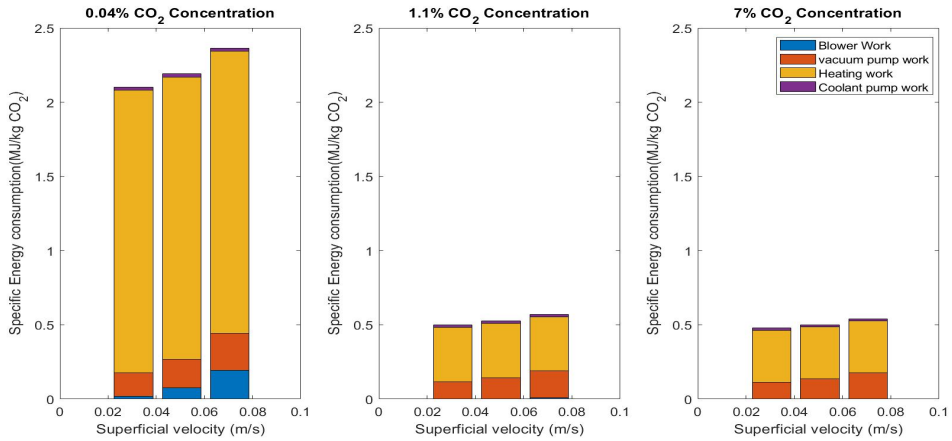

Figure 6.14: Specific energy consumed by model for varying superficial velocity

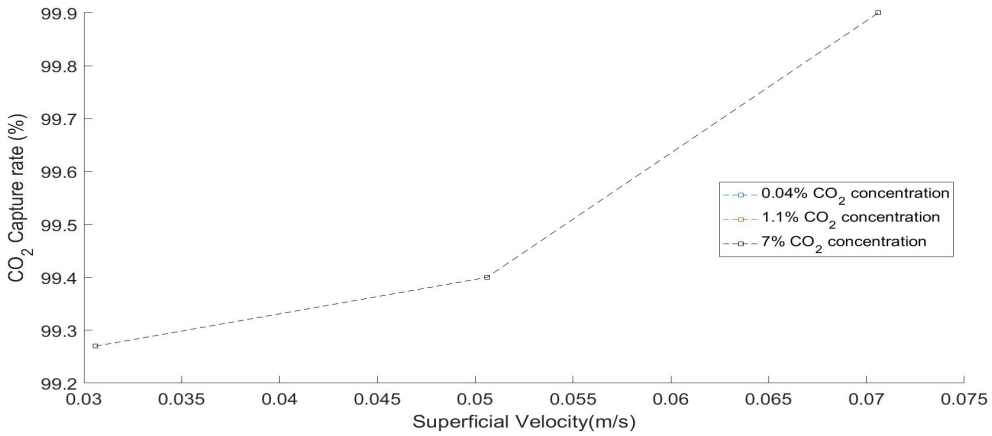

Figure 6.15: CO_2 capture rate of model for varying superficial velocity

6.3 Techno-economic analysis

The analysis is conducted initially with 1.1% CO_2 concentration with 87 t/h flue gas flow rate which is the concentration and flow of the manufacturing plant. Cost offset in this model is disregarded.

6.3.1 Absorption process

Techno-economic analysis for absorption process starts with the bare erected cost (BEC) shown in **table 6.2**. The scaled BEC for all the components except absorber column can be seen in **Table 6.2**. The key parameter used for scaling for each component is shown in **Table 6.1**.

Equipment	**S1 description**	**S1 (reference)**	**S2 (Model)**
Pellet reactor	Solvent flow rate in loop (t/h)	389000	1516
Calciner	$CaCO_3$ flow rate (t/h)	300	1,1762
Slaker	CaO flow rate (t/h)	165	0,6458
ASU	O_2 flow rate(t/h)	55,926	0,2384
CO2 Compressor	Electricity consumed (MW)	22	0,0785
Steam turbine	Electricity produced (kW)	9600	37,63
Fines Filter	$CaCO_3$ fines flow rate (t/h)	29,4	0,1285

Table 6.1: Absorption process BEC scaling key unit

Equipment	**Keith et.al. BEC (M$)[22]**	**Model scaled BEC (M$)**
Pellet reactor	76,9	3,07
Calciner	30,66	1,23
Slaker	13,14	0,53
ASU	38	1,60
CO_2 Compressor	17,2	0,65
Steam turbine	6,7	0,26
Fines Filter	17,6	0,75

Table 6.2: Absorption process BEC scaled values

Once the BEC is calculated, material cost(20% of BEC), labour cost(23%BEC), were added to it to get the total direct field cost (TDFC) the ratios for MC and LC were obtained from [15]. Next the indirect field cost (12.5% of TDFC [15]) is added to the TDFC to get the total field cost(TFC). Finally the contingency cost (20% of TFC[15]) and the engineering, procurement and construction cost (EPC) (17% of TFC[15]) is added to the TFC to get the total plant cost (TPC). All the costs are shown in **Table 6.3**.

CAPEX add ons	Value
BEC (M$)	10,7157
Material Cost (M$)	2,1532
Labour Cost (M$)	2,4560
TDFC (M$)	15,3249
Indirect field Cost (M$)	1,9432
TFC(M$)	17,2681
EPC (M$)	2,9694
Contingency(M$)	3,4536
TPC(M$)	23,6912
TPC(M€)	23,9281

Table 6.3: Absorption process TPC calculation with ASU

Next step was to find the replacement for the source of heat which was natural gas (100% CH_4 in the model. Techno-economic analysis was done to see what effects will the costs have when the ASU is replaced with an alkaline electroliser. [11] was used to generate the Cost function for BEC of the electrolyser which is 0.965 M€[11]. The TPC calculation for absorption process with electrolyser is shown in **Table 6.4**.

CAPEX add ons	Value
BEC (M$)	10,0807
Material Cost (M$)	2,0256
Labour Cost (M$)	2,3105
TDFC (M$)	14,4169
Indirect field Cost (M$)	1,8281
TFC(M$)	16,2450
EPC (M$)	2,7935
Contingency(M$)	3,2490
TPC(M$)	22,2875
TPC(M€)	22,5104

Table 6.4: Absorption process TPC calculation with alkaline electroliser replacing ASU

There are two operational costs(OPEX) that are taken into consideration for this model. Fixed OPEX and variable OPEX. The fixed OPEX is the cost of sorbent make up stream which is 26.26(€/t-CO_2) as shown in Keith et.al.[12]. The varying OPEX can also be called the energy cost which has two components to it, one is electricity cost(0.2717 €/kWh[15]) and the natural gas cost(3.535 €/GJ[15]).
For model where ASU is replaced with alkaline electroliser, the fixed OPEX cost for water(14.828 €/tCO2[11]) is added to generate the annual OPEX cost and the natural gas usage is negated. Additionally electricity is used for generating H_2 and heat.

6.3.2 Adsorption process

Since there is no enough data on the flows the BEC of the model is scaled up with amount of CO_2 adsorbed. The reference model is sized to capture 0.96 kt-CO_2/year. The model is up-scaled to capture 3.2558 kt-CO_2/year shown in **Table 6.5**. The installed cost and EPC cost is scaled up as per the reference[22].
The OPEX cost in this model is only dependent on variable OPEX cost which only has electricity cost at 0.2717 €/kWh[15]. The Cost results can be seen in the results section.

Equipment	**John Young et.al BEC M$ 0.96 kt/y**	**Scaled up model BEC (M$) 3.25 kt/y**	**Installed cost [M$]**	**Installed cost +EPC [M$]**
Bed	0,76	2,5776	3,8664	4,4425
Blower	0,433	1,4686	2,2645	2,6035
Vacuum Pump	0,0638	0,2164	0,3388	0,3900
Gas storage baloon	0,002	0,0068	0,0068	0,0078
Switching valves	1,19	4,0360	4,0360	4,6414
Sorbent	0,105	0,3561	0,3561	0,3561
Air source heat Pump	0,359	1,2176	1,2176	1,2176

Table 6.5: Adsorption process BEC scaled values

6.3.3 Cost comparison

For cost comparision the absorption model with alkaline electrolyser is used as it offsets the usage of natural gas and ASU. The comparitive results with ASU are added in the appendix. The reason for TPC of absorption process being costlier is mainly the BEC of pellet reactor(3,099 M€) which after the add on CAPEX cost increases to 6.85 M€. The unit that costs the most in adsorption model is the switching valves (4.64 M€). The TPC comparision of both the processes can be seen in **Figure 6.16**.

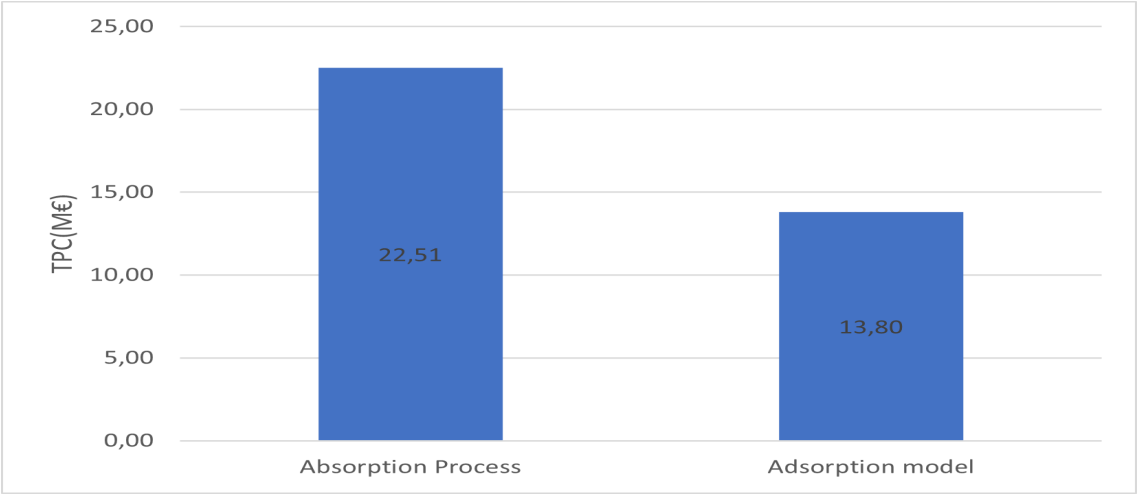

Figure 6.16: Total plant cost

The reason for comparatively higher OPEX cost of absorption process is due to electricity cost of the alkaline electroliser which alone has OPEX cost of 1.198 M€/year. The yearly OPEX cost comparision can be seen in **Figure 6.17**.

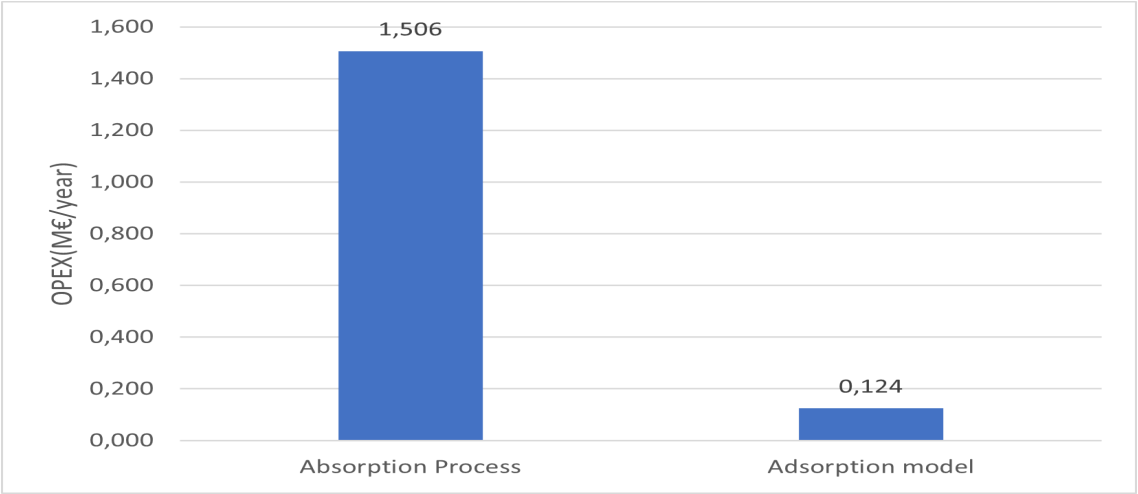

Figure 6.17: Yearly OPEX cost

When looking at the levelized cost of CO_2 captured, the resason for higher levelized CAPEX cost for absorption model is the same reason as the higher TPC. when coming to OPEX cost, the reason for higher cost in absorption process is the same

as higher yearly OPEX cost, which is mainly due to electricity consumption by electrolyser.

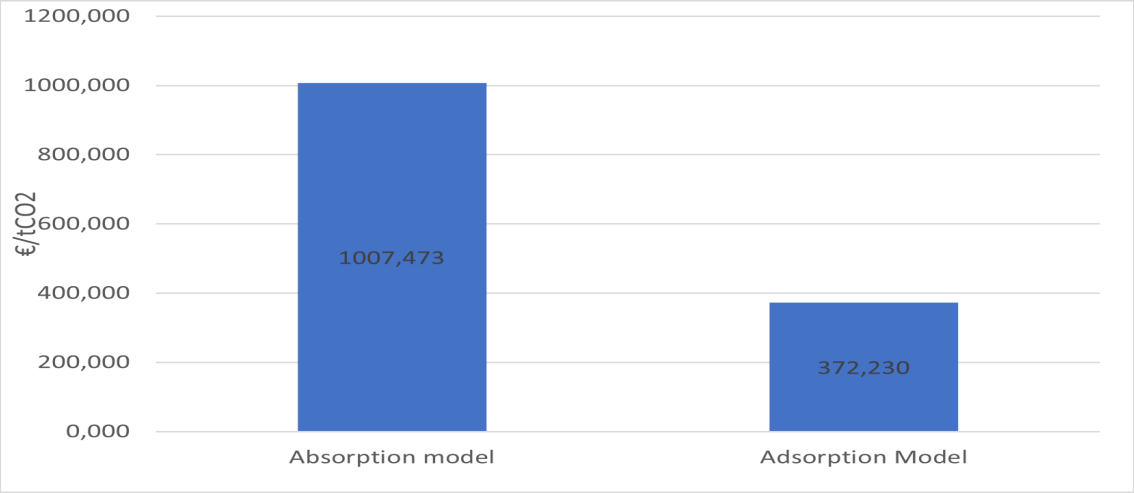

Figure 6.18: Levelized cost

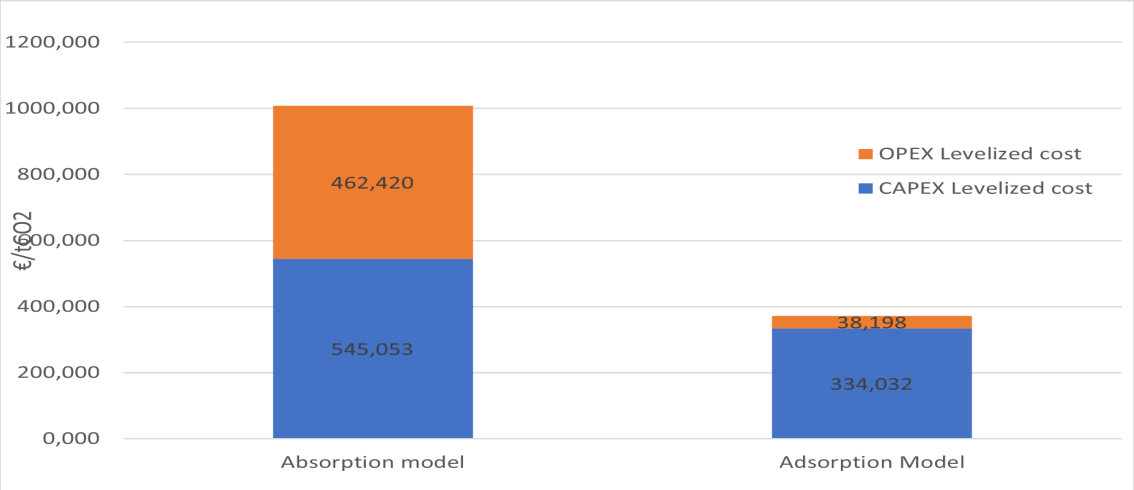

Figure 6.19: Levelized cost split

6.3.4 Techno-economic sensitivity analysis

Techno-economic sensitivity analysis of varying the CO_2 concentration keeping the flow rate constant at 87 t/h was conducted. From **Figure 6.20** and **Figure 6.22**, it can be seen that with increasing concentration of CO_2 in the flue gas the levelized cost for both adsorption and absorption process reduces. This due to increasing amount of CO_2 captured with increasing concentration. It is seen that TPC for both the processes increases with increase in concentration. This is because of increasing dimensions of all the components with increasing concentration for both the processes as seen in **Figure 6.21** and **Figure 6.23**. The reason for steep reduction in the cost levelized cost from the 0.04% case to 1.1% case is due to large increase in the amount of CO_2 captured. The reduction in rate of reduction of levelized cost from 1.1% to 7% shows that the advantage of up-scaling the plant size

with increasing the concentration evens out very quickly resulting in huge increase of TPC with little to no decrease in levelized cost.

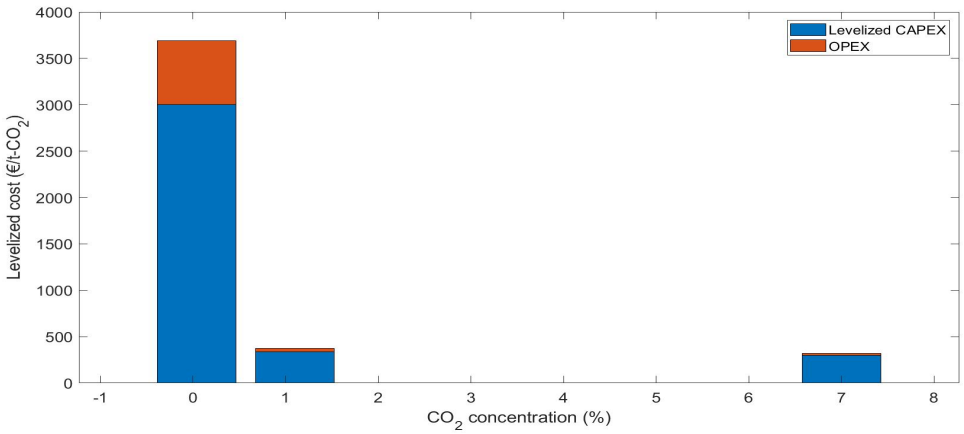

Figure 6.20: Levelized cost of adsorption process(varying concentration)

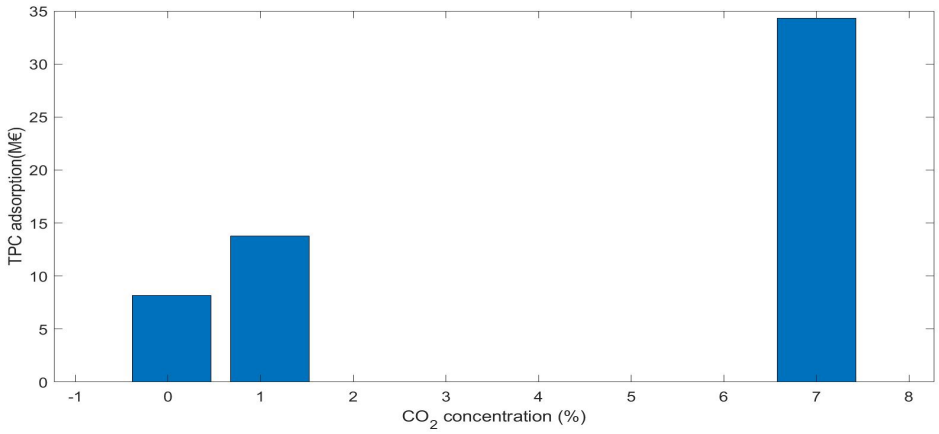

Figure 6.21: TPC of adsorption process(varying concentration)

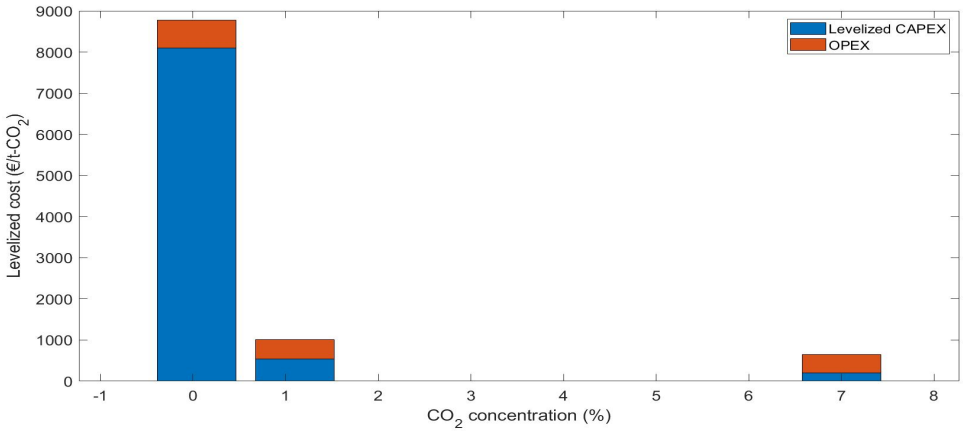

Figure 6.22: Levelized cost of absorption process(Varying concentration

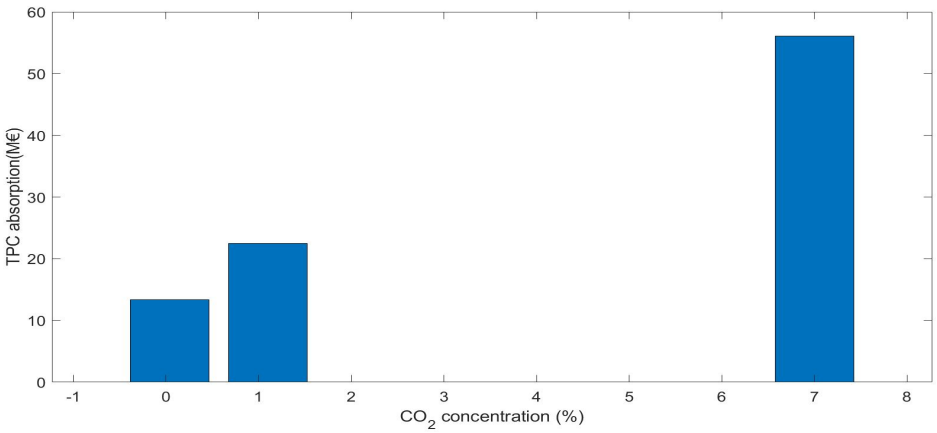

Figure 6.23: TPC of absorption process(varying concentration)

7
Conclusion

The main contribution of this work was to see how the specific energy consumption (GJ/tCO_2) varies with varying model parameters for both absorption and adsorption processes. In the absorption model as the concentration increased the specific energy consumed reduces(0.04%-1.1%) to a value after which it remains constant(1.2%-7%). With increasing capture rate the specific energy consumed decreases exponentially. Finally, it was seen that the specific energy consumed was not dependent on the flow rate of the flue gas and it remained constant.

In the adsorption model, with increasing column thickness the specific energy consumption decreases. With increasing desorption temperature the specific energy consumed increases. for varying CO_2 concentration in exhaust the specific energy consumed decreases at a very low rate when compared to decrease with increase in column thickness. Finally, the specific energy consumed increases with increase in superficial velocity. From the results it was seen that the higher energy consuming model between the two processes was the absorption model in all the scenarios this is in contrast with the DAC processes. This is due to increased energy consumption of absorber column in the absorption process.

From the techno-economic analysis it was seen that the TPC and the total levelized cost of the adsorption model (13.8 M€ & 372.23 €/tCO_2) was less when compared to the absorption process(22.51 M€ & 1007.47€/tCO_2). Based on the lower energy consumption and the lower TPC and levelized cost, it can be concluded that the cost effective and energy saving process out of the two DAC process for capture of CO_2 from a manufacturing plant would be the adsorption process. From the sensitivity analysis of techno-economics shows that the best set-up was to have the flue gas CO_2 concentration at 1.1% as we can see a huge drop in levelized cost of CO_2 capture. The levelized cost reduction advantage reduces with increasing the concentration to very high levels(7%) making the plant expensive.
The results from this thesis can be used to see which one of the two DAC process would work better for the manufacturing industry emitting flue gas with CO_2 concentration «4%.

7.1 Future work

- Running more scenarios for adsorption model.
- Developing detailed cost functions for techno-economic analysis to reduce the uncertainty.
- Modelling of alkaline electrolyser for the absorption process's calciner.

- Running more scenarios for techno-economic analysis to cover different concentrations.

Bibliography

[1] Aspen adsorption v12.1. 2021.

[2] Carbon dioxide now more than 50% higher than pre-industrial levels. 2022.

[3] Oumer Abduaziz, Jack Kie Cheng, Razman Mat Tahar, and Ramgopal Varma. A hybrid simulation model for green logistics assessment in automotive industry. *Procedia Engineering*, 100:960–969, 2015.

[4] Stefano Bianchi. Process modelling of a direct air capture (dac) system based on the kraft process, 2018.

[5] Maximilian Biermann, Christian Langner, Simon Roussanaly, Fredrik Normann, and Simon Harvey. The role of energy supply in abatement cost curves for co2 capture from process industry–a case study of a swedish refinery. *Applied Energy*, 319:119273, 2022.

[6] R Byron Bird, Warren E Stewart, Edwin N Lightfoot, and Robert E Meredith. Transport phenomena. *Journal of The Electrochemical Society*, 108(3):78C, 1961.

[7] Thomas Deschamps, Mohamed Kanniche, Laurent Grandjean, and Olivier Authier. Modeling of vacuum temperature swing adsorption for direct air capture using aspen adsorption. *Clean Technologies*, 4(2):258–275, 2022.

[8] Mahdi Fasihi, Olga Efimova, and Christian Breyer. Techno-economic assessment of co2 direct air capture plants. *Journal of cleaner production*, 224:957–980, 2019.

[9] Christoph Gebald. *Development of amine-functionalized adsorbent for carbon dioxide capture from atmospheric air*. PhD thesis, Eth Zurich, 2014.

[10] Christoph Gebald, Jan A Wurzbacher, Andreas Borgschulte, Tanja Zimmermann, and Aldo Steinfeld. Single-component and binary co2 and h2o adsorption of amine-functionalized cellulose. *Environmental science & technology*, 48(4):2497–2504, 2014.

[11] Dolf Gielen, Emanuele Taibi, and Raul Miranda. Hydrogen: A renewable energy perspective. *Abu Dhabi: International Renewable Energy Agency*, 2019.

[12] David W Keith, Geoffrey Holmes, David St Angelo, and Kenton Heidel. A process for capturing co2 from the atmosphere. *Joule*, 2(8):1573–1594, 2018.

[13] Zahra Rastegar and Ahad Ghaemi. Co2 absorption into potassium hydroxide aqueous solution: experimental and modeling. *Heat and Mass Transfer*, 58(3):365–381, 2022.

[14] Otto Redlich and Joseph NS Kwong. On the thermodynamics of solutions. v. an equation of state. fugacities of gaseous solutions. *Chemical reviews*, 44(1):233–244, 1949.

[15] Eloy S Sanz-Pérez, Christopher R Murdock, Stephanie A Didas, and Christopher W Jones. Direct capture of co2 from ambient air. *Chemical reviews*, 116(19):11840–11876, 2016.

[16] Ray Sinnott. *Chemical engineering design*, volume 6. Elsevier, 2014.

[17] Valentina Stampi-Bombelli, Mijndert van der Spek, and Marco Mazzotti. Analysis of direct capture of co 2 from ambient air via steam-assisted temperature–vacuum swing adsorption. *Adsorption*, 26(7):1183–1197, 2020.

[18] J Toth. State equation of the solid-gas interface layers. *Acta chim. hung.*, 69:311–328, 1971.

[19] Junwen Wang, Jingshan Li, and Ningjian Huang. Optimal vehicle batching and sequencing to reduce energy consumption and atmospheric emissions in automotive paint shops. *International Journal of Sustainable Manufacturing*, 2(2-3):141–160, 2011.

[20] Emmerich Wilhelm, Rubin Battino, and Robert J Wilcock. Low-pressure solubility of gases in liquid water. *Chemical reviews*, 77(2):219–262, 1977.

[21] John Young, Enrique García-Díez, Susana Garcia, and Mijndert Van Der Spek. The impact of binary water–co 2 isotherm models on the optimal performance of sorbent-based direct air capture processes. *Energy & Environmental Science*, 14(10):5377–5394, 2021.

[22] John Young, Noah McQueen, Charithea Charalambous, Spyros Foteinis, Olivia Hawrot, Manuel Ojeda, Hélène Pilorgé, John Andresen, Peter Psarras, Phil Renforth, et al. The cost of direct air capture and storage: the impact of technological learning, regional diversity, and policy. 2022.

[23] Yi Ge Zhang, Mark Pagani, Zhonghui Liu, Steven M Bohaty, and Robert DeConto. A 40-million-year history of atmospheric co2. *Philosophical Transactions of the Royal Society A: Mathematical, Physical and Engineering Sciences*, 371(2001):20130096, 2013.

A

Appendix 1

A.1 Absorption

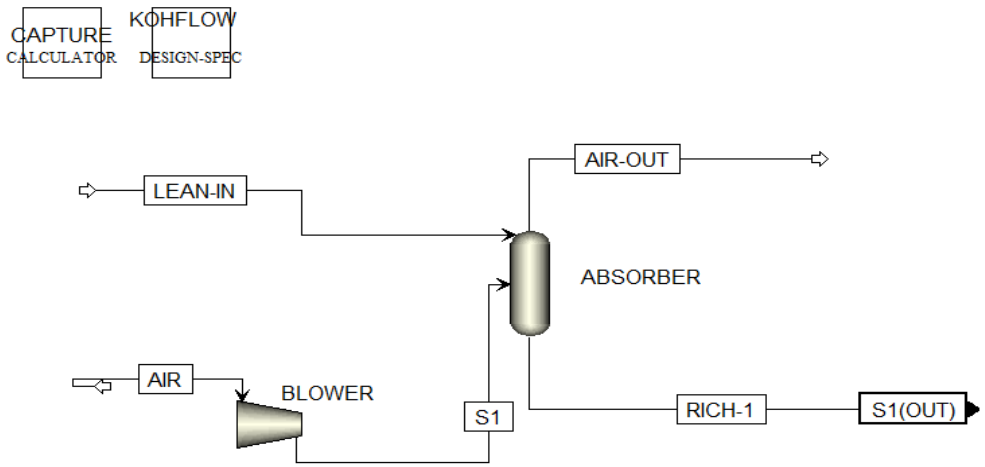

Figure A.1: Absorber hierarchy

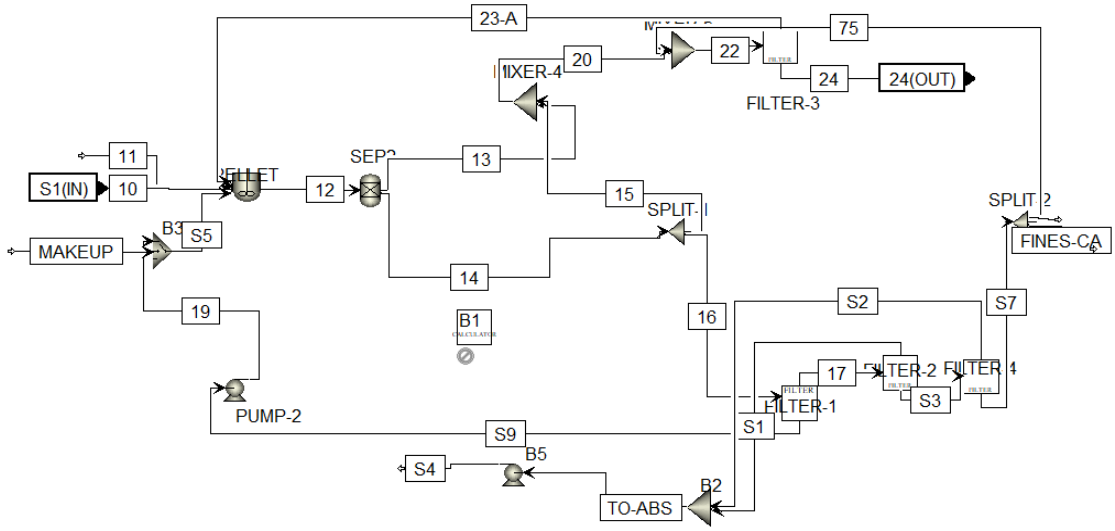

Figure A.2: Pellet reactor hierarchy

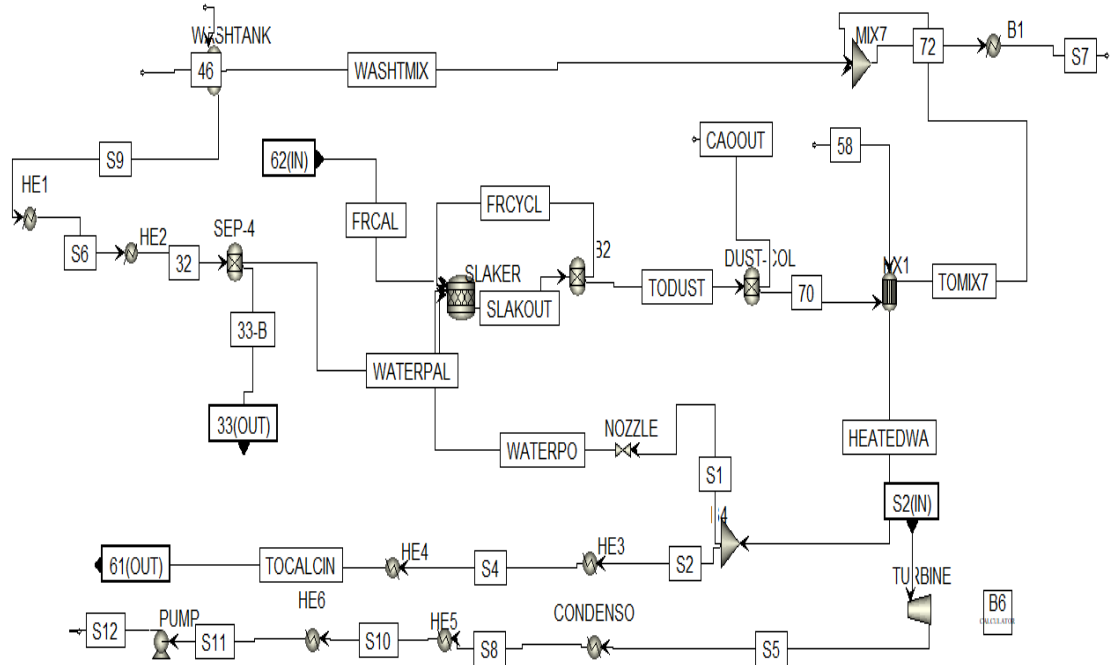

Figure A.3: Slaker hierarchy

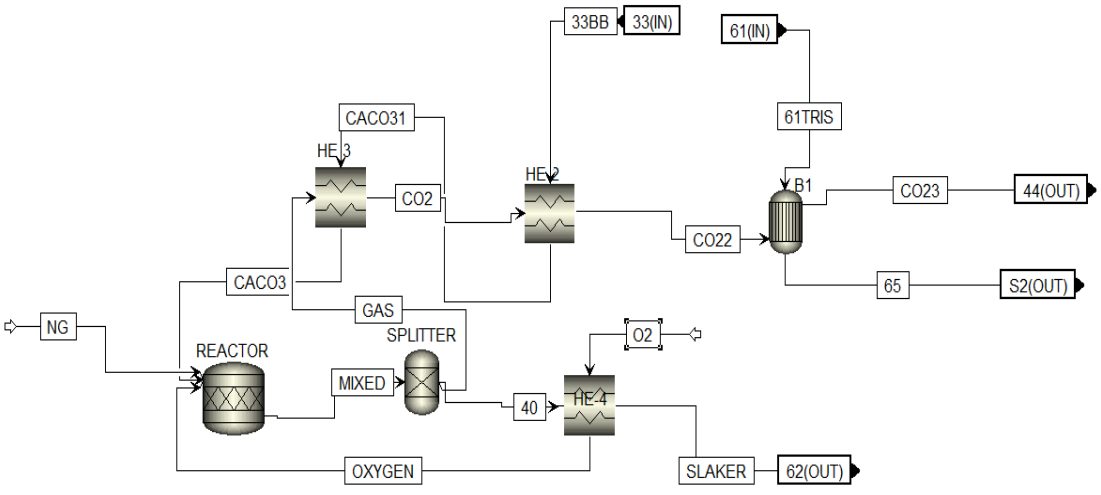

Figure A.4: Calciner hierarchy

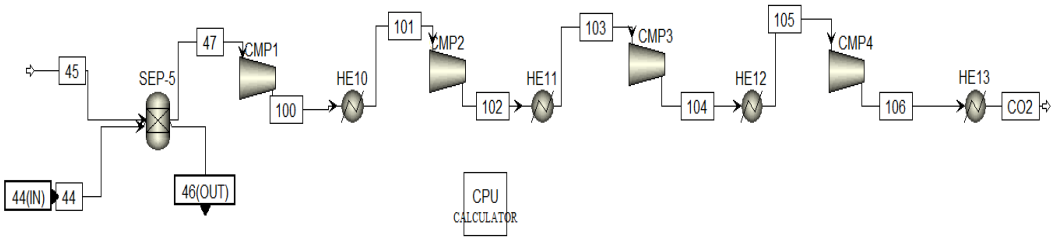

Figure A.5: Compressor hierarchy

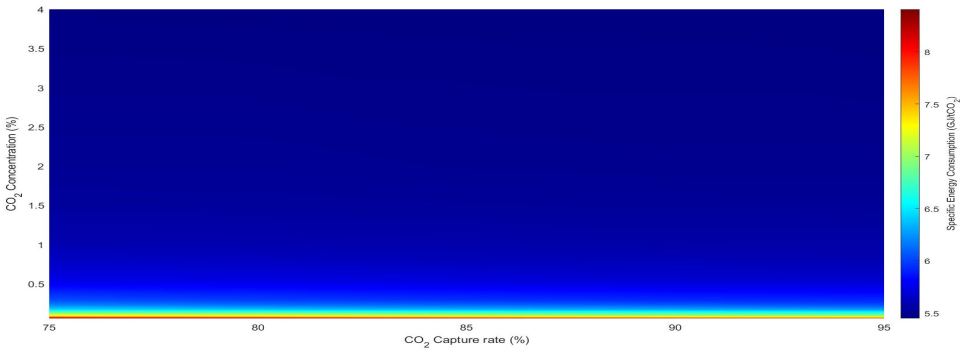

Figure A.6: Contour plot of absorption process

A.2 Adsorption

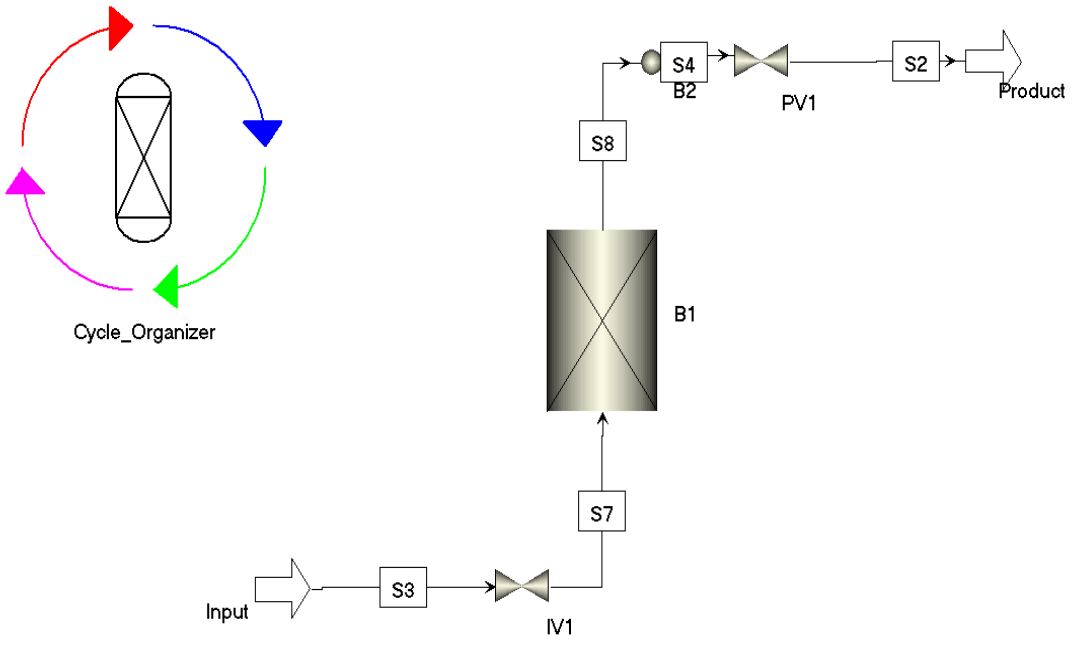

Figure A.7: Adsorption model

A.2.1 Isotherm code

This is the isotherm model code written in the System modeller language for GAB isotherm model and the Co-adsorption Toth isotherm.

```
CONSTRAINTS
  // Flowsheet variables and equations...
  Within B1.Layer(1).Isotherm(1).User_pPress_Isotherm(1)
  For i In FDESet Do
    //Binary GAB Isotherm for H2O adsorption
    W(i,"H2O")=(((IP(1,"H2O")*(EXP(1)^(((IP(2,"H2O")
    +(IP(3,"H2O")*T(i)))-(-44.38*T(i)+57220))/(8.314*
    T(i))))*(EXP(1)^(((IP(5,"H2O")-EXP(1)^(IP(6,"H2O")*
    T(i)))-(-44.38*T(i)+57220))/(8.314*T(i))))*((P(i)*
    Y(i,"H2O")*100000)/(611.21*EXP(1)^((18.678-((T(i)
    -273.15)/234.5))*((T(i)-273.15)/(T(i)-16.01))))))/
    ((1-((EXP(1)^(((IP(2,"H2O")+(IP(3,"H2O")*T(i)))-
    (-44.38*T(i)+57220))/(8.314*T(i))))*((P(i)*Y(i,"H2O")
    *100000)/(611.21*EXP(1)^((18.678-((T(i)-273.15)/234.5))*
    ((T(i)-273.15)/(T(i)-16.01))))))*(1+((EXP(1)^((
    (IP(5,"H2O")-EXP(1)^(IP(6,"H2O")*T(i)))-(-44.38*
    T(i)+57220))/(8.314*T(i))))-1)*(EXP(1)^(((IP(2,"H2O")
    +(IP(3,"H2O")*T(i)))-(-44.38*T(i)+57220))/(8.314*T(i))))
    *((P(i)*Y(i,"H2O")*100000)/(611.21*EXP(1)^((18.678-
    ((T(i)-273.15)/234.5))*((T(i)-273.15)/(T(i)-16.01)))))))))/1000);
    // Co-Adsorption Toth Isotherm for CO2 adsorption
    W(i,"CO2")=(((IP(1,"CO2")*EXP(1)^(0*(1-T(i)/
    IP(2,"CO2"))))*(1/(1-(-0.137*W(i,"H2O")*1000))))*(IP(4,"CO2")
    *EXP(1)^(IP(5,"CO2")/(8.314*T(i)))*(1+5.612*W(i,"H2O")*1000))*
    (P(i)*Y(i,"CO2")*100000))/((1+((IP(4,"CO2")
    *EXP(1)^(IP(5,"CO2")/(8.314*T(i)))*(1+5.612*W(i,"H2O")*
    1000))*(P(i)*Y(i,"CO2")*100000))^(IP(7,"CO2")+
    (IP(8,"CO2")*(1-IP(2,"CO2")/T(i)))))^(1/(IP(7,"CO2")
    +(IP(8,"CO2")*(1-IP(2,"CO2")/T(i)))))*1000);
    W(i,"N2")=(IP(1,"N2")*IP(2,"N2")*1)/
    (1+((IP(2,"N2")*1)^(IP(3,"N2"))))^(1/IP(3,"N2"));
  EndFor
EndWithin
END
```

A.3 Techno-economic comparison

The following images show the techno-econnomic comparative results of absorption process with ASU in place of alkaline electrolyser and the adsorption process.

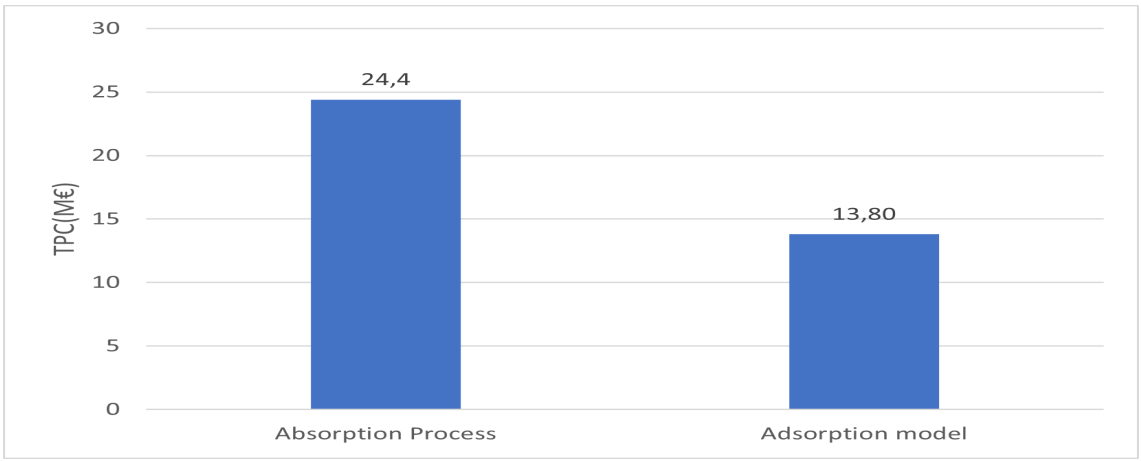

Figure A.8: TPC comparision

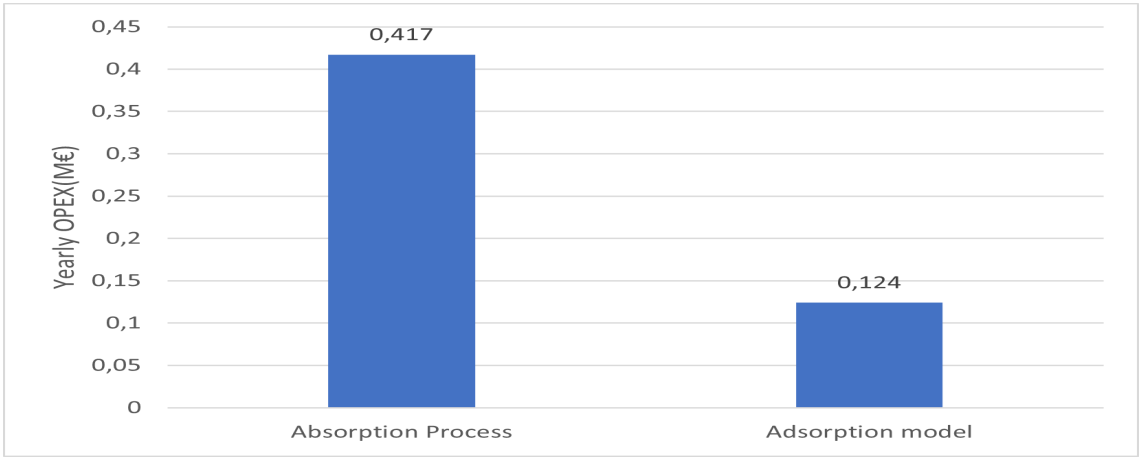

Figure A.9: Yearly OPEX cost comparison)

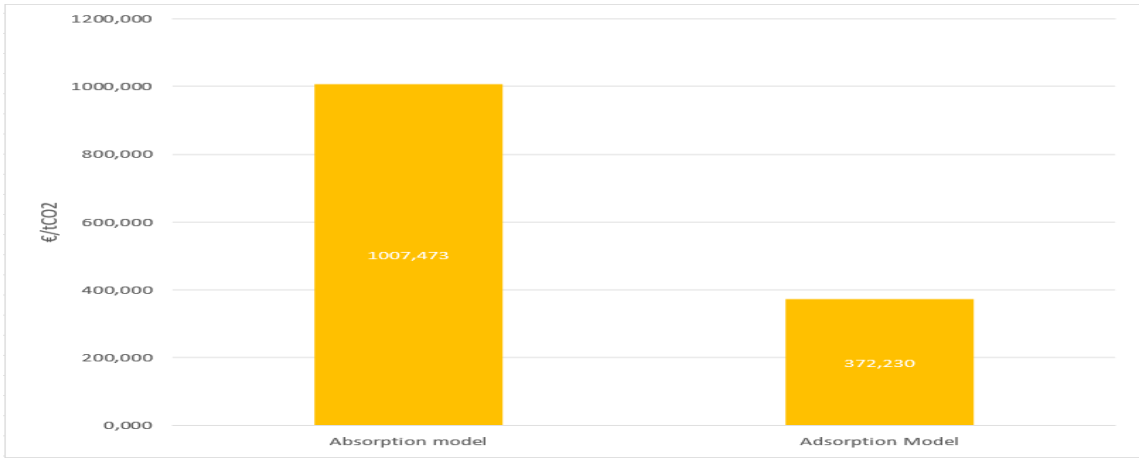

Figure A.10: Total levelized cost comparison

DEPARTMENT OF SOME SUBJECT OR TECHNOLOGY
CHALMERS UNIVERSITY OF TECHNOLOGY
Gothenburg, Sweden
www.chalmers.se

CHALMERS
UNIVERSITY OF TECHNOLOGY